BRAIN
ORIGINAL ARTICLE

Anti-pan-neurofascin antibodies induce subclass-related complement activation and nodo-paranodal damage

Luise Appeltshauser,[1] Helena Junghof,[1] Julia Messinger,[1] Janis Linke,[1,2] Axel Haarmann,[1] Ilya Ayzenberg,[3,4] Panoraia Baka,[5] Johannes Dorst,[6] Anna L. Fisse,[3] Thomas Grüter,[3] Valerie Hauschildt,[7] Alexander Jörk,[8] Frank Leypoldt,[9,10] Mathias Mäurer,[11] Edgar Meinl,[12] Sebastian Michels,[6] Jeremias Motte,[3] Kalliopi Pitarokoili,[3] Mark Stettner,[13] Carmen Villmann,[14] Marc Weihrauch,[15] Gabriel S. Welte,[16] Inga Zerr,[7,17] Katrin G. Heinze,[2] Claudia Sommer[1] and Kathrin Doppler[1]

Autoimmune neuropathy associated with antibodies against pan-neurofascin is a new subtype of nodo-paranodopathy. It is relevant because it is associated with high morbidity and mortality. Affected patients often require intensive care unit treatment for several months, and data on the reversibility and long-term prognosis are limited. The pathogenicity including IgG subclass-associated mechanisms has not been unravelled, nor directly compared to anti-neurofascin-155 IgG4-related pathology. Understanding the underlying pathology might have a direct impact on treatment of these severely affected patients. By a multicentre combined prospective and retrospective approach, we provide clinical data of a large cohort of patients with anti-neurofascin-associated neuropathy ($n = 18$) including longitudinal titre and neurofilament light chain assessment via Ella® and relate clinical data to *in vitro* pathogenicity studies of anti-neurofascin antibodies. We assessed antibody binding characteristics and the pathogenic effects of anti-pan-neurofascin versus neurofascin-155 antibodies on living myelinating dorsal root ganglia co-cultures. Additionally, we analysed the IgG subclass profile and the complement binding capacity and effector functions considering the effects of intravenous immunoglobulin preparations via enzyme-linked immunosorbent and cell-based assays.

In contrast to chronic neurofascin-155 IgG4-associated neuropathy, anti-pan-neurofascin-associated disease presented with a high morbidity and mortality, but as a monophasic and potentially reversible disorder. During follow-up, antibodies were no longer detectable in 8 of 11 patients. Anti-pan-neurofascin had direct access to the nodes of Ranvier in myelinating cultures titre-dependently, most probably inducing this severe phenotype. Antibody preincubation led to impaired paranode formation, destruction of paranodal architecture and alterations on paranodal myelin and sensory neurons in the cultures, with more severe effects than neurofascin-155 antibodies. Besides IgG4, subclass IgG3 was detected and associated with complement binding and cytotoxic effects *in vitro*. As a possible correlate of axonal damage *in vivo*, we detected highly increased serum neurofilament light chain levels (sNF-L), correlating to serum C3a. Still, sNF-L was not identified as a marker for poor prognosis, but rather as an intra- and interindividual marker for acuteness, severity and course, with a strong decrease during recovery.

Our data provide evidence that anti-pan-neurofascin antibodies directly attack the node and induce severe and acute, but potentially reversible, nodo-paranodal pathology, possibly involving complement-mediated mechanisms. Screening for autoantibodies thus is crucial to identify this subset of patients who benefit from early antibody-depleting therapy. Titre and sNF-L might serve as valuable follow-up parameters. The prospect of a favourable outcome has high relevance for physicians, patients and relatives during months of critical care.

Received June 18, 2022. Revised September 29, 2022. Accepted October 20, 2022. Advance access publication November 8, 2022

1 Department of Neurology, University Hospital of Würzburg, 97080 Würzburg, Germany
2 Rudolf Virchow Center, Center for Integrative and Translational Bioimaging, Julius Maximilian University of Würzburg, 97080 Würzburg, Germany
3 Department of Neurology, St. Josef Hospital Bochum, Ruhr University of Bochum, 44791 Bochum, Germany
4 Department of Neurology, I.M. Sechenov First Moscow State Medical University, 119146 Moscow, Russia
5 Department of Neurology, University Medical Center of the Johannes Gutenberg University, 55131 Mainz, Germany
6 Department of Neurology, University Hospital Ulm, 89081 Ulm, Germany
7 Department of Neurology, University Medical Center Göttingen, 37075 Göttingen, Germany
8 Hans Berger Department of Neurology, Jena University Hospital, 07747 Jena, Germany
9 Neuroimmunology Section, Institute of Clinical Chemistry, University Hospital Schleswig-Holstein, Kiel/Lübeck, Germany
10 Department of Neurology, Kiel University, 24105 Kiel, Germany
11 Department of Neurology, Klinikum Würzburg Mitte gGmbH, Standort Juliusspital, 97070 Würzburg, Germany
12 Institute of Clinical Neuroimmunology, Biomedical Center and University Hospital, Ludwig Maximilian University of Munich, 82152 Planegg, Germany
13 Department of Neurology, University Hospital of Essen, 45147 Essen, Germany
14 Institute for Clinical Neurobiology, University Hospital Würzburg, 97080 Würzburg, Germany
15 Department of Neurology, Bundeswehrkrankenhaus Ulm, 89081 Ulm, Germany
16 Department of Neurology, KRH Klinikum Nordstadt, 30167 Hannover, Germany
17 German Center for Neurodegenerative Diseases, 37075 Göttingen, Germany

Correspondence to: Luise Appeltshauser
Department of Neurology
University Hospital of Würzburg
Josef-Schneider-Strasse 11, 97080 Würzburg, Germany
E-mail: Appeltshau_L@ukw.de

Keywords: autoantibodies; complement; neurofascin; neurofilament light chain; nodo-paranodopathy

Introduction

Guillain–Barré syndrome (GBS) is an acute immune-mediated neuropathy with potentially high morbidity and mortality.[1] Patients present with disabling symptoms including rapid progressive, sensorimotor tetraparesis, autonomic and cranial nerve involvement and at times respiratory insufficiency. Still, the pathophysiology and the clinical phenotypes are heterogeneous, imposing great challenges on clinical management.[1,2]

In a subset of patients initially classifying as GBS, IgG autoantibodies directed against adhesion molecules of the node of Ranvier can be detected. Targets are contactin-1 and contactin-1 associated protein (Caspr-1), gliomedin and nodal and paranodal isoforms of neurofascin.[3–7] Despite a frequent acute to subacute onset, IgG4 antibodies often associate with a chronic neuropathy, formerly classified as acute-onset chronic inflammatory demyelinating polyradiculoneuropathy (CIDP).[8–13] Due to its growing impact, distinct clinical features and distinct pathophysiology compared to GBS or CIDP, autoimmune neuropathies with nodal or paranodal antibodies were recently categorized as a distinct entity termed autoimmune nodopathy.[14,15] The pathogenicity of antibodies against neurofascin-155 and contactin-1 has been shown in various studies.[10,16–19] Their detection has direct implications on diagnostic work-up and clinical management of seropositive patients, who respond poorly to standard therapy but well to rituximab.[14,15]

Most recently, a shared epitope on different nodo-paranodal neurofascin isoforms 140/155/186 (pan-neurofascin) has been identified as a target in acute-onset immune-mediated neuropathy.[12,20] As the disease is rare, anti-pan-neurofascin seropositive patients have only been described at low numbers or even in single case studies.[12,20–27] A distinct clinical phenotype has been proposed in this subset: they present with a severe, GBS-like onset and after initial short recovery, develop a fulminant course of disease with tetraplegia, autonomic instability, cranial nerve involvement, respiratory failure with prolonged ventilation, insufficient response to standard treatment and a high mortality.[12,20,21,26,27]

So far, knowledge on anti-pan-neurofascin-associated neuropathy is mostly restricted to clinical data. Nevertheless, these reports of single patients with prolonged but partly reversible and monophasic course imply different pathogenic mechanisms compared to chronic anti-neurofascin-155-IgG4-mediated neuropathy. Remarkably, anti-pan-neurofascin antibodies can be of the IgG1/3 subclass.[12,20,26] Unlike IgG4, IgG1/3 can trigger Fc-mediated effector functions including cross-linking and complement activation, possibly mediating complement-associated pathologies.[28,29] Hence, the subclass-related *in vitro* and *in vivo* role of complement needs further attention. Furthermore, the isoform-dependent accessibility of nodo-paranodal targets to autoantibodies may contribute to their pathogenic effect, but has not been investigated so far.

In this study, we included a large cohort of patients with definite anti-pan-neurofascin antibodies. We aimed at typifying the clinical phenotype including long-term serological and clinical follow-up and direct comparison to anti-neurofascin-155 seropositive including the assessment of serum neurofilament light chain (sNF-L) as a biomarker for axonal damage at nadir and during follow-up. We quantitatively assessed IgG subclasses, complement binding and effector functions under influence of intravenous immunoglobulin preparations, and analysed binding characteristics of the antibodies and pathogenic effects in comparison to neurofascin-155 using myelinating co-cultures, thus providing a detailed clinical

and pathophysiological characterization of this rare but severe disease.

Materials and methods

Patients

Patients with definite anti-neurofascin antibodies (further referred to as 'seropositive') were identified from a cohort of patients who underwent diagnostic testing for anti-paranodal antibodies (see Supplementary material). Clinical data were collected retrospectively from patient records in seropositive patients and prospectively once they had been identified. In 14 of the 18 seropositive patients, follow-up serum samples were available [total $n = 31$, mean follow-up period 16.6 (3–48) months, see Supplementary Table 1]. Healthy control sera of 10 controls from previous studies[6,30] were used for the experimental procedures. Patients and controls whose sera were used for the experiments had given written informed consent. The study was approved by the Ethics Committee of the Medical Faculty, University of Würzburg (reference number 278/13, 15/19 and 220/20).

Antibody detection

We performed antibody screening via enzyme-linked immunosorbent assay (ELISA) and binding assays on murine teased fibres[10,20,31] including serum-specific normalization[6,32] in all patients as previously described. Positivity was confirmed in cell-based assays with human embryonic kidney cells (HEK293) transfected with human neurofascin-155 and -186 and murine neurofascin-140[33] as previously reported (for antibodies see Supplementary Table 2).[20,31] Only patients positive both in ELISA and cell-based assay were enrolled. Neurofascin-155 ELISA was used for antibody titre assessment via dilution series (1:100–1:40 000) and subclass analysis at a serum dilution of 1:100 as previously described.[6]

Titre-adjusted ELISA including immunoglobulin preincubation

In order to quantitatively compare IgG subclasses, complement C1q binding and the effects of intravenous immunoglobulin preparations (IVIg), the dilution of the sera was adjusted to the antibody titre as previously described[30] and validated as described in the Supplementary material and Supplementary Fig. 1. Subclass ELISA was performed as described in detail in the Supplementary material. To study possible neutralizing effects of IVIg preparations on antigen epitopes and soluble anti-neurofascin IgG, we performed anti-neurofascin-155 ELISA with IVIg preincubation. Mean optical density (OD) values of 14 patients were included in the analysis. Privigen® Immune Globulin Intravenous (Human) 10% Liquid (CSL Behring, King of Prussia) was preincubated in separate assays in a dilution series of 0.78 mg/ml to 25 mg/ml either (i) before the addition of the serum or (ii) preincubated with the sera before addition to the ELISA plate, using bovine serum albumin (BSA; Merck KGAa/EMD) dilution series as a separate control. The following steps and analysis were performed as previously described.[1] In order to assess possible neutralization of antigen-specific binding sites, $F(ab')_2$ fragments of neurofascin-155-specific IgG were generated and validated as previously described[34] using Pierce $F(ab')_2$ Preparation Kit (#44988, Thermo Fisher Scientific) for neurofascin-155-positive patient 12. Titre-specific dilution of the generated $F(ab')_2$ fragments was determined (1:7.5) and validated (see Supplementary Fig. 1). IVIg/BSA preincubation was performed with $F(ab')_2$ fragments of patient 12 and a seronegative control.[34]

ELISA- and cell-based complement C1q binding and cytotoxicity

The ELISA-based C1q binding assay was performed as previously described,[1] but with modifications as described in the Supplementary material. HEK293 cells were cultivated and transfected with neurofascin-155 plasmids as previously described.[4,5] Fixation, washing and blocking were followed by a 2-h preincubation of sera with anti-pan-neurofascin and anti-neurofascin-155 and control sera at titre-adjusted dilution. After washing, we added complement C1q (Merck) diluted 200 µg/ml for 1 h at room temperature. Double immunofluorescence staining was performed using Cy3™-conjugated anti-human IgG and FITC-conjugated rabbit anti-C1q (see Supplementary Table 2). Slides were assessed using a LSM 980 microscope with Airyscan 2 (Zeiss) with equal settings for image acquisition. Complement-mediated cytotoxicity including the effects of IVIg was assessed on neurofascin-155-transfected HEK293 cells using Cytotoxicity Detection KitPLUS (LDH) Version 06 (Roche Diagnostics GmbH) following the manufacturer's instructions in a modified protocol similar to previously reported[9] and described in the Supplementary material.

Serum biomarker assessment

Serum neurofilament light chain (sNF-L) levels were assessed in sera of seropositive patients ($n = 17$, one patient excluded due to lack of material), follow-up sera if available ($n = 30$) and an equal number of healthy control sera using an equivalent of Simoa™,[35] Ella SimplePlex™ assay[36] for the detection of human NF-L (SPCKB-PS-002448, ProteinSimple, Bio-Techne). CSF was not available for testing. Serum C3a concentrations (ng/ml) were measured in eight healthy control sera, nine sera with anti-pan-neurofascin, six sera with anti-neurofascin-155 and 14 follow-up sera using Invitrogen Complement C3a Human ELISA Kit (BMS2089, Thermo Fisher Scientific).

Serum and purified IgG preincubation on murine myelinating dorsal root ganglion explant cultures

Murine myelinating organotypic dorsal root ganglion (DRG) neuron/Schwann cell explant co-cultures were established using a modified protocol from Taveggia *et al.* and Stettner *et al.*[37,38] (see Supplementary material). Formation of heminodes was achieved at Day 12, formation of full node and paranodes at Day 16 of cultivation (see Supplementary material).

To assess binding to the nodes of Ranvier, sera of five healthy controls, six patients with anti-neurofascin-155 and eight patients with anti-pan-neurofascin antibodies patients diluted 1:100 in myelination medium were preincubated for 24 h on the myelinating co-cultures at Day 16.

To assess the influence of anti-paranodal antibodies on node and paranode formation in the culture system, we incubated serum diluted 1:100 and purified IgG with equal amounts of neurofascin-specific IgG (see Supplementary material, Supplementary Table 3 and Supplementary Fig. 1) from Day 12, before complete paranode formation. We used samples of a control and two patients with anti-pan-neurofascin and neurofascin-155 serum with equal titres (1:10 000), incubated for 5 days with daily changes of serum/IgG/medium. To assess long-term pathological changes on more mature nodes of Ranvier in the culture system, 5-day preincubation

was started at Day 16. The assays were repeated thrice for each condition in independent experiments with equal culture, staining and imaging conditions (exception for purified IgG started at Day 12, see Supplementary material).

Cells were then fixated and triple immunostaining was performed either with anti-human IgG in combination with anti-myelin-associated glycoprotein (MAG) and commercial anti-pan-neurofascin (to assess serum binding) or with nodo-paranodal marker antibodies (Caspr-1, neurofascin-186, pan-neurofascin, pan-sodium channel) in combination with anti-MAG to assess long-term pathologies as described in detail in the Supplementary material. Three colour photomicrographs including 63-fold magnification and large field-of view multi-tile images at a 20-fold magnification were assessed with confocal microscopy using the LSM 980 with Airyscan 2. Quantitative image analysis including node of Ranvier morphometrics was performed by a blinded researcher as described in the Supplementary material.

Statistical analysis

We used SPSS Statistics version 28.0.0 (IBM) and Prism V9.3.0 (GraphPad Software, San Diego, CA, USA). Tests used in the assays are described in the Supplementary material and figure legends. Graphs were created with Prism/Illustrator (Adobe Inc., San José, CA, USA) and schematic illustrations were created with BioRender.com.

Data availability

The data that support the findings of this study are available from the corresponding author, upon reasonable request.

Results

Antibodies against neurofascin isoforms in patients with inflammatory neuropathies

We detected and confirmed antibodies against neurofascin in 18 patients with inflammatory neuropathies (see Supplementary Fig. 2). Eleven patients showed reactivity against all three isoforms of neurofascin (140/155/186) and seven against isoform neurofascin-155 only. Titres ranged from 1:100 to 1:30 000 (see Supplementary Table 1).

Clinical characteristics of seropositive patients

We found significant differences in the phenotype of anti-pan-neurofascin compared to anti-neurofascin-155 seropositive patients (see Table 1 and Supplementary Table 1). Anti-pan-neurofascin seropositive patients were older and showed a severe, GBS-like phenotype with acute onset, severe sensorimotor tetraparesis, cranial nerve involvement, partially locked-in syndrome (5/11 patients) and autonomic instability. Morbidity was high, with intermediate/intensive care treatment in nine patients, assisted ventilation with prolonged ventilation time (mean 26 ± 14.4 weeks) in six patients and a mortality of 18% (2/11 patients). Clinical scores such as the Medical Research Council (MRC) sum score,[39] Overall Disability Sum Score[40] (ODSS) and the Guillain–Barré Syndrome Disease Severity score[41] (GBS-DS) were significantly worse in anti-pan-neurofascin seropositive patients. Most importantly, anti-pan-neurofascin patients had a prolonged and severe but monophasic course of disease. Neurofascin-155 patients, in contrast, showed the typical features of chronic neurofascin-155 IgG4-associated nodo-paranodopathy, such as a young age, severe sensorimotor involvement, tremor and sensory ataxia.

There were no significant differences in treatment response in the two groups (see Table 1, Supplementary Table 1 and Supplementary Fig. 3): most patients showed an initial but not persistent response to IVIg. Importantly, anti-pan-neurofascin patients initially improved significantly under IVIg treatment, but had a quick and fulminant relapse within a few days to weeks. Response to plasmapheresis was partial, and response to corticosteroids poor. In the anti-pan-neurofascin group, three of four patients showed remission even without antibody-depleting therapy. One patient with low-titre anti-pan-neurofascin had remission without having received rituximab, another patient not having received rituximab developed chronic, but stable disease. Long-term response to antibody-depleting therapy with rituximab was very efficient in both groups, leading to a titre decrease and clinical improvement. Dosage and treatment regimen of rituximab treatment were heterogeneous within the cohort. Treatment regimen was chosen according to the treating physician's recommendation, considering clinical presentation and antibody titre, as common guidelines do not include recommendation on dosing.[14] Rituximab dosage and intervals are listed in detail in Supplementary Table 1 and shown in Supplementary Fig. 3. In neurofascin-155-associated disease, remission was achieved after repeated rituximab treatments in two patients, but three patients needed further repetitive rituximab treatment. Follow-up after the last cycle of rituximab treatment was 13 (6–24) months in pan-neurofascin-positive patients and 11 (0–20) months in neurofascin-155 patients. Despite prolonged treatment intervals, all five anti-pan-neurofascin patients who had received rituximab remained seronegative during follow-up, with good outcome (see Supplementary Video 1 for outcome and Supplementary Fig. 3 for individual treatment-related titres).

Complement-binding IgG3 subclass as a unique feature of anti-pan-neurofascin

We compared the IgG subclass profile of anti-pan-neurofascin versus anti-neurofascin-155 seropositive sera via ELISA with titre-adjusted dilutions (see Supplementary Fig. 1). Anti-pan-neurofascin seropositive patients showed high OD_{450nm} values for IgG3, whereas anti-neurofascin-155 patients were negative for IgG3 subclass (median 1.71 versus 0.06, $P = 0.002$). OD_{450nm} of IgG2 subclass was significantly lower in the anti-pan-neurofascin subcohort (median 0.37 versus 2.89, $P = 0.007$). IgG4 was present in all patients of both groups (see Fig. 1A). Subclass profiles did not change during the disease course.

Using an ELISA-based and titre-adapted complement C1q binding assay, we found mean C1q OD_{450nm} values to be significantly increased in anti-pan-neurofascin compared to anti-neurofascin-155 (1.96 ± 1.03 versus 0.54 ± 0.41, $P = 0.013$; see Fig. 1B). We detected a positive correlation of C1q OD_{450nm} values with OD_{450nm} values of IgG3, but not with any other subclass ($r = 0.83$, adjusted $P = 0.013$; see Fig. 1C). The presence of IgG3 subclass therefore seems to be a unique feature of anti-pan-neurofascin-associated nodo-paranodopathy and leads to complement C1q binding.

Effects of IVIg preparations on antibody and complement binding

We assessed the effects of IVIg preparations on antibody and complement binding *in vitro* as illustrated in Fig. 2. We did not find any

Table 1 Clinical characteristics of anti-neurofascin seropositive patients

Clinical feature	Pan-neurofascin	Neurofascin-155	P-value [test]	OR	95% CI
Descriptive statistics					
Number of patients	$n = 11$	$n = 7$			
Sex, male/female	9/2	5/2	0.61[a]	1.80	0.22–13.83
Mean age at onset ± SD	61.2 ± 15.8	42.0 ± 21.5	0.044[b]		
Clinical presentation					
Antecedent infection	4/9 (44.4%)	2/6 (33.3%)	0.67	1.60	0.15–11.52
Time to nadir < 4 weeks	7/11 (63.6%)	0/7 (0%)	0.007[a]	∞	2.05–∞
Mean time to nadir (weeks)	5.4 ± 5.2	20.0 ± 16.0	0.036[c]		
Symmetric distribution	10/11 (90.9%)	6/7 (85.7%)	0.73[a]	1.67	0.08–34.40
Proximal and distal distribution	7/11 (63.5%)	5/7 (71.4%)	0.73[a]	0.70	0.10–5.61
Sensory ataxia	5/11 (45.5%)	4/7 (57.1%)	0.63[a]	0.63	0.11–4.14
Tremor	0/11 (0%)	4/7 (57.1%)	0.004[a]	0.00	0.00–0.58
Neuropathic pain	3/11 (27.3%)	3/7 (42.9%)	0.49[a]	0.50	0.09–3.05
Cranial nerve involvement	9/11 (81.8%)	0/7 (0%)	<0.001[a]	∞	4.14–∞
Locked-in like syndrome	6/11 (54.6%)	0/7 (0%)	0016 [a]	∞	1.43–∞
Autonomic instability	6/11 (54.5%)	2/7 (28.6%)	0.28[a]	3.00	0.45–19.07
IMC/ICU treatment	9/11 (81.8%)	0/7 (0%)	<0.001[a]	∞	4.14–∞
Assisted ventilation	6/11 (54.6%)	0/7 (0%)	0.016[a]	∞	1.43–∞
Mean hospitalization time (weeks)	27.3 ± 22.6	2.2 ± 2.3	0.03[c]		
Clinical scores (nadir)					
Mean GBS-DS ± SD	4.5 ± 1.4	2.6 ± 1.0	0008[b]		
Median ODSS (range)	10.3 (3–12)	5.4 (3–9)	0.007[c]		
Median MRC sum score (range)	0 (0–60)	50 (34–56)	0.007[c]		
Diagnostic assessment					
Mean CSF cell count/µl ± SD	2.4 ± 3	3.8 ± 2	0.33[b]		
Median CSF protein in mg/dl (range)	917.5 (298–7680)	1466 (523–4397)	0.28[c]		
MRI cauda equina enhancement	2/7 (28.6%)	2/4 (50%)	0.48[a]	0.40	0.04–4.32
Treatment response					
PE response (initial)	6/11 (54.5%)	6/6 (100%)	0.049[a]	0.00	0.00–1.29
PE response (permanent)	5/11 (45.5%)	2/6 (33.3%)	0.63[a]	1.67	0.20–11.33
IVIg response (initial)	6/10 (60%)	5/7 (71.4%)	0.63[a]	0.60	0.09–5.01
IVIg response (permanent)	2/10 (20%)	2/7 (28.6%)	0.68[a]	0.63	0.08–5.13
Corticosteroids (initial)	1/7 (14.3%)	2/5 (40%)	0.31[a]	0.25	0.01–3.19
Corticosteroids (permanent)	1/7 (14.3%)	1/5 (20%)	0.79[a]	0.67	0.03–15.58
Rituximab (initial)	6/6 (100%)	5/5 (100%)	n.a.	n.a.	n.a.
Rituximab (permanent)	4/5 (80%)	5/5 (100%)	0.29[a]	0.00	0.00–9.00
Outcome					
Acute deterioration/deceased	2/11 (18.2%)	0/7 (0%)	0.23[a]	∞	0.30–∞
Stabilization/improvement—chronic	1/9 (11.1%)	5/7 (71.4%)	0.013[a]	0.05	0.00–0.68
Remission (with residues)—monophasic	8/9 (88.9%)	2/7 (28.6%)	0.013[a]	20.0	1.47–256.5

Descriptive statistics, clinical presentation, results of diagnostic assessment and frequencies of treatment response and outcome are shown in the subcohort of patients with anti-pan-neurofascin (column 2) and anti-neurofascin-155 (column 3). Results of statistical testing comparing the two cohorts are shown in the last three columns. ICU = intensive care unit, IMC = intermediate care, IVIg = intravenous immunoglobulins, n.a. = not applicable, PE = plasma exchange.

[a]Asymptotic chi-square test.

[b]Student's *t*-test.

[c]Mann–Whitney U-test.

evidence that IVIg preparations blocked neurofascin antigen epitopes, as the patients' mean OD values in the ELISA were stable when adding a dilution series of IVIg to the coated protein compared to addition of a control protein (see Fig. 2C). Furthermore, OD values were stable when preincubating IVIg with all patients' soluble antibodies (Fig. 2D) and with purified IgG $F(ab')_2$ fragments of patient 12 (mean relative $OD_{no\ Ig/25mgml\ IVIg} = 1.00$, data not shown), thus arguing against an antibody-neutralizing effect of IVIg.

Next, we studied possible Fc-masking effects of IVIg by adding an IVIg preparation dilution series in the complement C1q binding assay before incubation of C1q. Here, we detected a slight although not significant reduction of the mean OD values (see Fig. 2E). In contrast, when preincubating IVIg with soluble C1q complement, we detected a significant and dose-dependent reduction of the OD compared to the control protein preincubation (see Fig. 2F), thus arguing in favour of a C1q neutralizing effect of IVIg.

Complement-mediated cytotoxicity of anti-pan-neurofascin

To investigate complement-related effector functions, we assessed C1q binding on neurofascin-155 transfected HEK293 cells. We detected binding of C1q colocalizing with anti-human IgG on cells that were previously incubated with anti-pan-neurofascin seropositive serum (see Fig. 3A). We did not detect C1q binding when preincubating with anti-neurofascin-155 or with healthy control sera (see Fig. 3B and C).

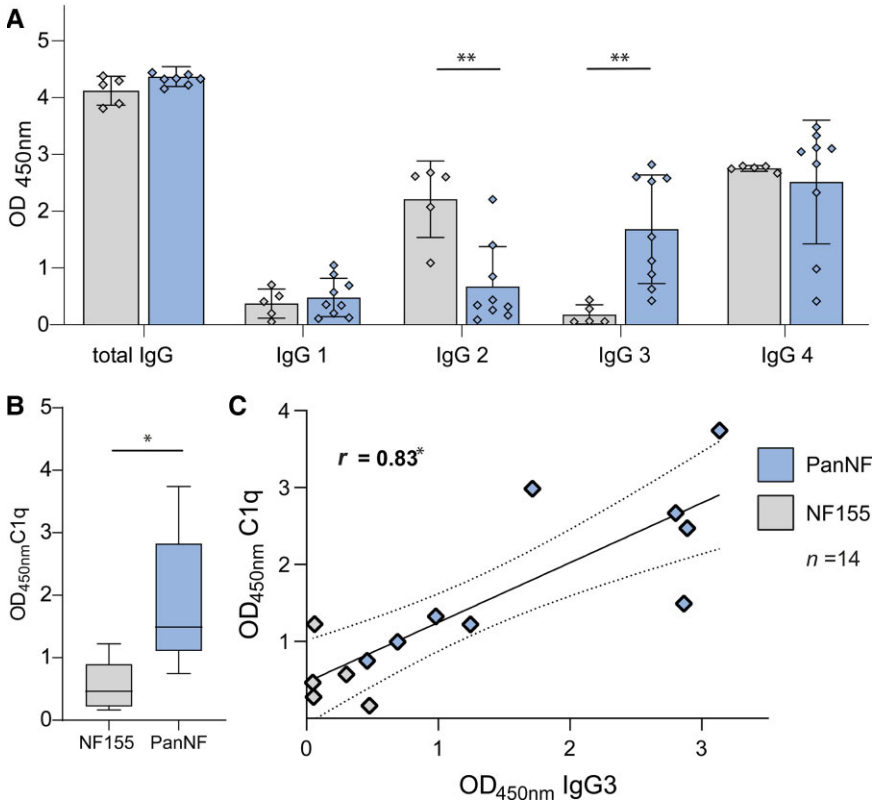

Figure 1 ELISA subclass profile and C1q IgG binding. (**A**) Mean OD_{450nm} in ELISA including standard deviations (error bars) and individual values. We used titre-adjusted sera of nine anti-pan-neurofascin and five anti-neurofascin-155 seropositive patients and secondary antibodies against human IgG ('total IgG') and titrated subclass-specific IgG1, IgG2, IgG3 and IgG4 secondary antibodies. Medians were compared using Mann–Whitney U-test, significant differences are highlighted by asterisks (see below). (**B**) Box-and-whisker plot showing median (line), first and third quartiles (box) and min/max values (whiskers) of OD_{450nm} of C1q binding of single patients' means. We compared the neurofascin-155 cohort versus the pan-neurofascin using two-sided *t*-test, significant differences are highlighted by asterisks (see below). (**C**) The scatter dot chart including simple linear regression (line) with 95% confidence intervals (dotted lines) illustrates a significant correlation of the OD_{450nm} of C1q binding with the OD_{450nm} of the IgG3 subclass ELISA in patients with anti-pan-neurofascin and anti-neurofascin-155. Significance level: $^{*}P < 0.05$, $^{**}P < 0.01$.

Next, we measured lactate dehydrogenase (LDH) release on transfected HEK293 cells that had been incubated with five sera each of anti-pan-neurofascin, anti-neurofascin-155 patients and controls in combination with standard complement serum. Relative cytotoxicity was increased in anti-pan-neurofascin preincubation compared to control preincubation (adjusted $P = 0.004$) and anti-neurofascin-155 preincubation (adjusted $P = 0.017$; see Fig. 3D). The relative cytotoxicity in seropositive patients correlated to the OD_{450} of C1q binding ($r = 0.67$, $P = 0.04$; see Fig. 3E). We studied the effects of IVIg preparations in the cell-based assay exemplarily, using two sera of the patients with the highest complement-mediated relative cytotoxicity. We could detect a significant reduction of the cytotoxicity by IVIg in two repeated assays (mean rel. cytotoxicity = 4.3% versus 14.1%, $P = 0.0129$; see Fig. 3F). Thus, only anti-pan-neurofascin serum bound and activated complement, leading to cell lysis *in vitro* and being influenced by IVIg.

Nodo-paranodal accessibility in a living cell culture model

To assess the binding of serum antibodies to the nodo-paranodal region, the surrounding Schwann cells and sensory neurons *in situ*, we performed serum binding assays to living myelinated DRG neurons, using triple immunofluorescence for human IgG in combination with nodo-paranodal and myelin markers.

We did not detect any specific binding of the control sera to the nodo-paranodal region (see Fig. 4A). In five anti-neurofascin-155 seropositive patients with high titres (1:2500–1:14 000), we detected only slight IgG depositions around the paranodes (see Fig. 4B). Double immunofluorescence with commercial anti-pan-neurofascin after fixation and permeabilization showed that neurofascin was not internalized or depleted during the preincubation period. However, there was no exact colocalization of commercial pan-neurofascin and human IgG deposits at the paranodes, arguing in favour of a low accessibility of anti-neurofascin-155 antibodies to the paranodes *in situ*. In contrast, we detected strong binding of anti-neurofascin-155 sera to the Schwann cell surface of myelinating Schwann cells and staining of the outer mesaxon (see Fig. 4C and Supplementary Video 2). One patient with a neurofascin-155-titre of 1:100 did not show any specific binding.

In four anti-pan-neurofascin seropositive patients with high titres (1:1000–1:30 000), we detected strong binding to the nodal region of the node of Ranvier, flanked by light paranodal depositions and co-localizing with the nodal fraction of commercial pan-neurofascin, but not completely with the paranodal fraction (see Fig. 4D and Supplementary Video 2). Four patients with low titres (1:100–1:500) did not show any specific binding.

Thus, because of its exposed localization at the nodal region, neurofascin-186 as a target is far more accessible to pathogenic

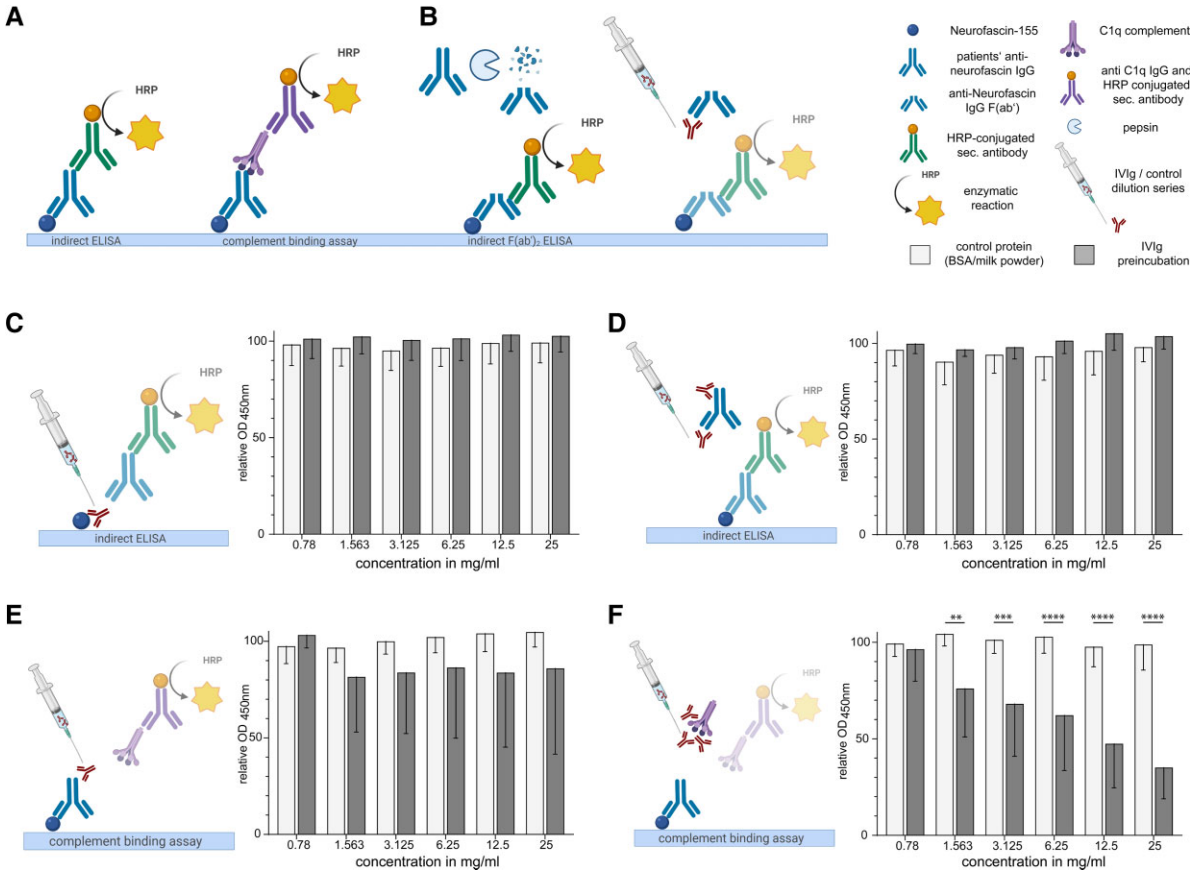

Figure 2 Effects of IVIg in ELISA and complement binding assay. (**A** and **B**) schematic display of the (**A**) ELISA and ELISA-based C1q complement binding assay, (**B**) generation of F(ab′)$_2$ fragments in patient 12 and ELISA with preincubation of IVIg with F(ab′)$_2$. All patients' mean relative OD to an IVIg/BSA/milk powder concentration of 0 mg/ml are displayed with standard deviations in bar graphs using a IVIg/BSA/milk powder dilution series from 0.78 to 25 mg/ml. (**C**) No reduction of antibody binding was detected when preincubating the bound antigen with IVIg. (**D**) No reduction of antibody binding was detected when preincubating soluble antibodies with IVIg. (**E**) A slight but not significant reduction of mean C1q OD levels was noted when preincubating IVIg with antigen-bound IgG antibodies in the C1q binding assay. (**F**) IVIg incubation has C1q neutralizing effects, with a significant reduction of relative ODs in a dose-dependent manner, when preincubating IVIg with C1q before addition to the assay. Statistical testing was performed using paired *t*-test and Wilcoxon signed rank test, depending on normal distribution of the data. Significance level: $^{*}P < 0.05$, $^{**}P < 0.01$, $^{***}P < 0.001$, $^{****}P < 0.0001$. Schematic display created with BioRender.com.

autoantibodies *in situ* than paranodal neurofascin-155, and binding strongly depends on the autoantibody titre.

Destruction of the nodo-paranodal architecture by neurofascin antibodies

We assessed pathogenic effects of anti-neurofascin antibodies on living myelinating co-cultures. Therefore, we performed long-term serum and purified IgG preincubation before and after node of Ranvier formation and qualitatively assessed morphological alterations. Furthermore, we quantified the results by triple staining with nodo-paranodal count and morphometrics on high-resolution large field of view photomicrographs (Fig. 5A and B and Supplementary Video 3).

When incubating serum containing anti-neurofascin during the myelination process, we observed an impaired formation of nodes of Ranvier, with even more severe effects after anti-pan-neurofascin compared to anti-neurofascin-155. Control serum preincubation did not have effects on node of Ranvier formation. In controls, we observed a high number of intact nodes of Ranvier in myelinated DRG explants (see Fig. 5G). Neurofascin was expressed at the nodes and paranodes, and Caspr-1 at the paranodes (Fig. 5A and C). In contrast, the median number of intact nodes per myelinated fibre was reduced after anti-neurofascin preincubation (controls: 1091 versus anti-neurofascin-155: 561 versus anti-pan-neurofascin: 211 nodes/mm² myelinated fibre, $P = 0.0073$; see Fig. 5G). Paranodal Caspr-1 staining was lost partially or even completely, and a dispersion of Caspr-1 along the axon was observed (see Fig. 5B and C). The nodal gap was significantly elongated (controls: 1.55 versus anti-neurofascin-155: 1.90 versus anti-pan-neurofascin: 3.08 µm, $P < 0.0001$ each; see Fig. 5K). In cultures incubated with anti-pan-neurofascin, neurofascin expression was mostly restricted to the nodes and no longer expressed at the paranodes, resulting in a shortened median neurofascin length due to paranodal degradation of neurofascin-155 (controls: 2.77 versus anti-neurofascin-155: 2.31 versus anti-pan-neurofascin: 1.74 µm, $P < 0.0001$; see Fig. 5I). Incubation with purified IgG led to morphological alterations comparable to serum preincubation.

When incubating cultures with patients' serum after the formation of nodes of Ranvier, we observed similar effects, again more severely with anti-pan-neurofascin compared to anti-neurofascin-155. Caspr-1 was lost partially and paranodal neurofascin-155 was lost almost completely after pan-neurofascin incubation. This

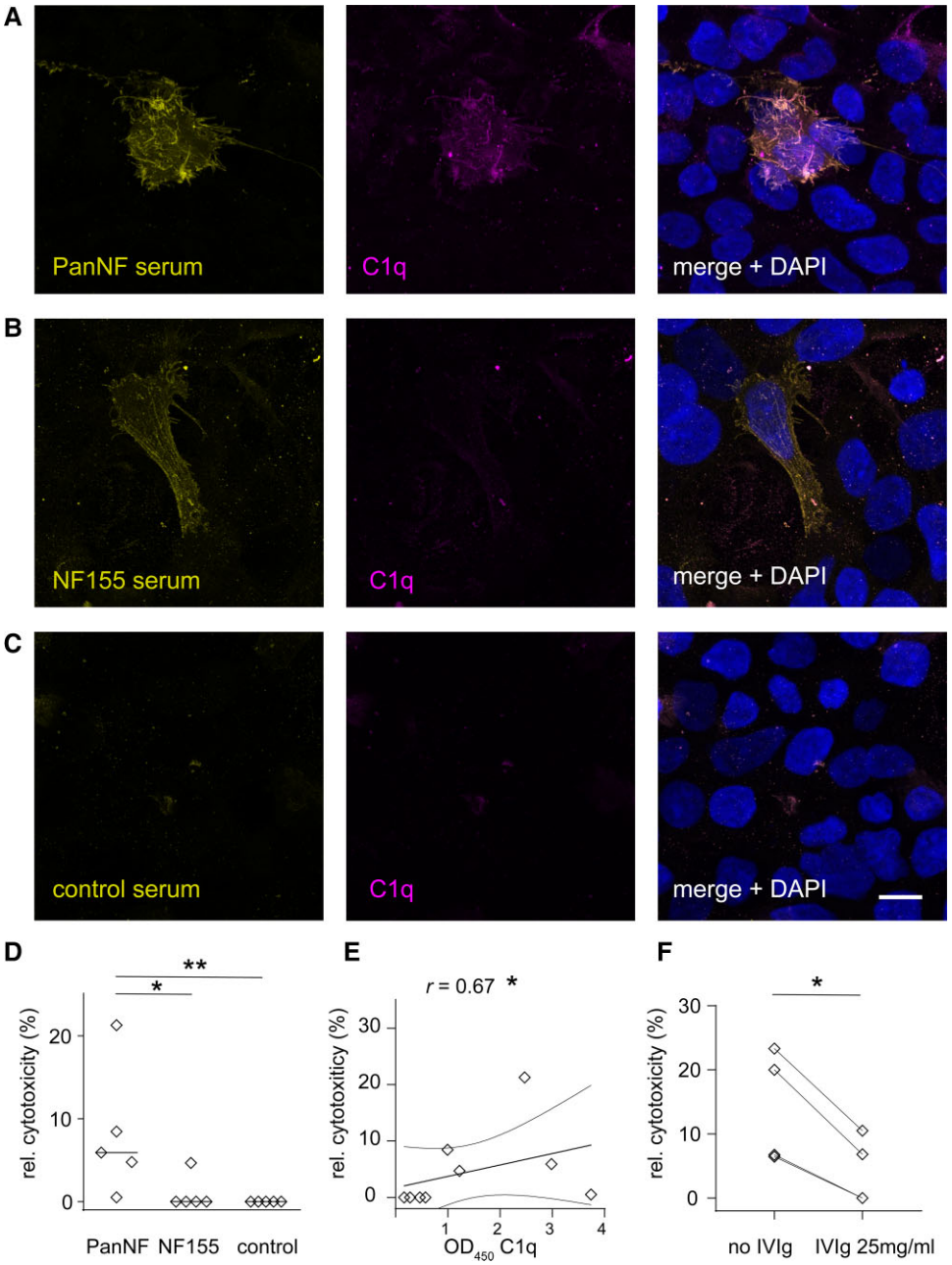

Figure 3 Complement binding and effects in the cell-based assay. (**A–C**) Photomicrographs of neurofascin-155 (NF155) transfected HEK293 cells incubated with serum and complement factor C1q and triple immunostaining with anti-human IgG (yellow), anti-C1q (magenta) and DAPI (blue). Incubation with serum containing anti-pan-neurofascin (PanNF) antibodies leads to complement C1q deposition on transfected cells (**A**), whereas no complement deposition was observed using serum with NF155 antibodies (**B**) or serum of a healthy control (**C**). Scale bar = 10 µm. (**D**) The relative cytotoxicity measured by LDH assay and calculated according to instructions of the manufacturer is displayed in percent (%) for preincubation of five sera with anti-PanNF, NF155 antibodies and healthy control sera. Kruskal–Wallis test with Dunn's correction for multiple testing was used for statistical testing. (**E**) The scatter dot chart illustrated the Spearman correlation of the relative cytotoxicity (%, *y*-axis) with the OD_{450nm} of the C1q binding assay in seropositive patients. (**F**) The mean relative cytotoxicity (%) is displayed in two patients with anti-PanNF antibodies without and with IVIg co-incubation with complement serum. Two-sided paired *t*-test was used for comparison. Significance level: $^{*}P < 0.05$, $^{**}P < 0.01$. rel. = relative.

resulted in a highly shortened median length of stained neurofascin (controls: 5.45 versus anti-neurofascin-155: 4.93 versus anti-pan-neurofascin: 2.91 µm, $P < 0.0001$; see Fig. 5J). Again, the median nodal gap was broadened (controls: 1.27 versus anti-neurofascin-155: 1.82 versus anti-pan-neurofascin: 2.51 µm, $P < 0.0001$; see Fig. 5L). The median total nodo-paranodal Caspr-1 length was increased after anti-pan-neurofascin preincubation (controls: 6.24 versus anti-pan-neurofascin: 6.51 µm, $P = 0.0077$), arguing in favour of a lateral dispersion of Caspr-1. After anti-pan-neurofascin serum preincubation, we did not observe this effect (6.35 µm with high variance, n.s.; see Fig. 5H), possibly due to a simultaneous degradation/loss of Caspr-1 at the

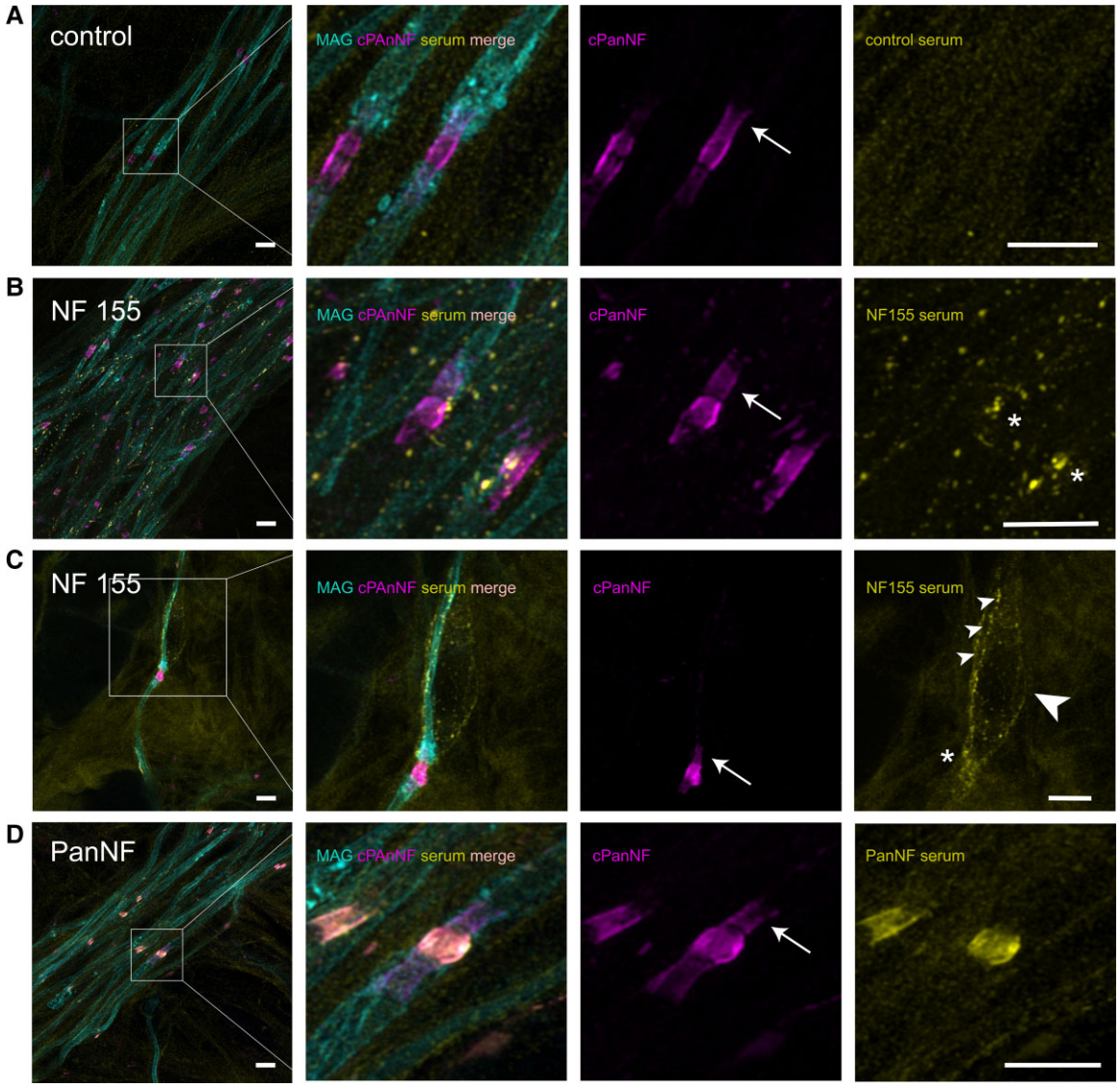

Figure 4 Nodo-paranodal accessibility in a living cell culture model. Photomicrographs including high magnification of myelinated fibres and nodes of Ranvier in dorsal root ganglia/Schwann cell explant co-cultures are shown after serum preincubation of a healthy control serum (**A**), serum of a patient with neurofascin-155 (NF155) antibodies (**B** and **C**) and with pan-neurofascin (PanNF) antibodies (**D**). Myelin associated glycoprotein (MAG)-staining is shown in cyan, commercial pan-neurofascin in magenta and serum IgG in yellow. (**A**) After preincubation with a control serum, no specific IgG deposition at the paranodes was observed. (**B** and **C**) After preincubation with NF155 serum, we did not observe a perfect colocalization of commercial antibody against neurofascin and IgG at the paranodes, but just flanking paranodal IgG deposits as indicated by asterisk. Furthermore, we observed specific IgG deposits at the outer myelin sheath (small arrowheads) and at Schwann cell bodies of myelinating Schwann cells (big arrowheads). (**D**) After preincubation with anti-PanNF-serum, strong IgG deposition was found at the node, co-localizing with the commercial nodal fraction of PanNF and thus neurofascin-186 isoform. No deposits were observed at the paranodes (arrows). Scale bar = 5 µm.

paranode.[19] The control serum preincubation did not alter nodo-paranodal morphometrics compared to direct fixation and staining without preincubation (median total neurofascin length 5.45 versus 5.37 µm, $P = 0.90$ n.s. and nodal length 1.49 versus 1.67 µm, $P = 0.57$).

To assess anti-pan-neurofascin specific changes at the nodal region, we performed triple staining with commercial pan-neurofascin, neurofascin-186 and pan-sodium antibodies and observed broadening of the nodal gap and slight dispersion of neurofascin-186 and sodium channels, but without complete loss of the two proteins, which still co-localized perfectly (see Supplementary Fig. 4).

Incubation with purified IgG had similar effects on nodo-paranodal architecture compared to serum preincubation, if assessed qualitatively. We observed a reduced number of nodes, (partial) loss of Caspr-1 and neurofascin-155 at the paranode, dispersion of paranodal proteins and nodal lengthening. In direct morphometrical comparison, the total neurofascin length and the nodal gap length were not significantly different when using serum versus IgG of patients with anti-neuroascin-155 as well as controls. Using anti-pan-neurofascin serum versus IgG, morphometrics differed slightly, indicating more severe degradation of pan-neurofascin and nodal gap lengthening when using serum instead of purified IgG (see Supplementary Fig. 5).

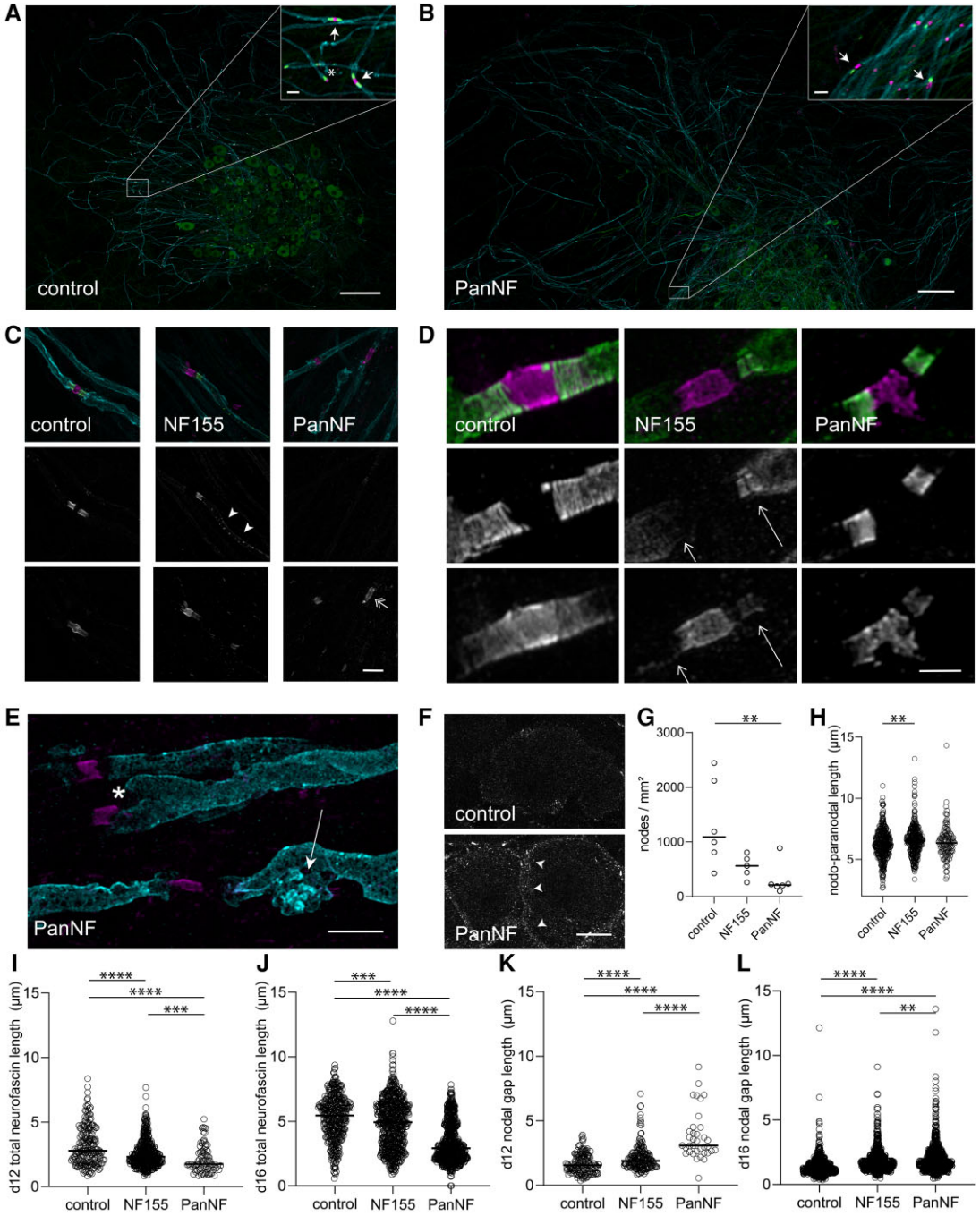

Figure 5 Effects of serum containing anti-neurofascin antibodies on living myelinating co-cultures. (**A** and **B**) Triple immunostaining [Caspr-1: green; MAG: cyan; anti-pan-neurofascin (Pan NF): magenta] after 5-day serum preincubation during node of Ranvier (NOR) formation. **A** shows intact NOR formation (arrowheads) and heminodes (asterisk) after control preincubation. **B** shows incomplete NOR formation with Caspr-1 hemistaining despite complete myelination and elongated nodes (arrow) after anti-PanNF preincubation. Scale bar = 100 µm, inlet = 5 µm. (**C**) High magnification of preincubation during myelination with overlay photomicrographs (first row) and single-channel photomicrographs (Caspr-1, PanNF) shows healthy NOR formation after control preincubation (*left*), partial loss and dispersion of Caspr-1 (arrowheads) after neurofascin-155 (NF155) preincubation and a complete loss of Caspr-1 and paranodal neurofascin and nodal elongation (double arrow) after anti-PanNF preincubation. Scale bar = 5 µm. (**D**) Double immunofluorescence after serum preincubation on already formed NOR. Anti-NF155 preincubation (*middle*) leads to a destruction of already formed paranodes with partial loss of paranodal NF155 and Caspr-1 (simple arrows) and a nodal elongation. Preincubation with anti-PanNF serum (*right*) leads to destruction of both paranodal and nodal neurofascin and nodal elongation. Scale bar = 2 µm. (**E**) Myelin alterations (MAG, cyan) after anti-pan-neurofascin preincubation with paranodal swelling (asterisk) and myelin balls (arrow). Scale bar = 5 µm. (**F**) Neurofascin-186 overexpression at the sensory neuron membrane after anti-PanNF preincubation (curved arrowheads). Scale bar = 10 µm. (**G**) Count of intact NOR per segmented MAG area in mm^2 shows reduction of intact nodes after anti-PanNF preincubation. (**H**) Nodo-paranodal length (Caspr-1 staining) after serum preincubation during and after NOR formation. (**I** and **J**) The total neurofascin length after preincubation during NOR (**I**) and after NOR formation (**J**) gives evidence of (partial) degradation of neurofascin after serum anti-neurofascin preincubation. (**K** and **L**) Nodal gap (Caspr-1 gap) length was significantly elongated after serum preincubation during (**K**) and after (**L**) NOR formation. Statistical testing was performed using Kruskal–Wallis test with Dunn's correction for multiple testing.

Furthermore, we observed morphological alterations of myelin after anti-pan-neurofascin serum and IgG incubation. Analysing MAG staining, we noted paranodal swelling and formation of myelin balls (see Fig. 5E and Supplementary Fig. 6). Schmidt-Lanterman incisures expressing neurofascin-155 could only be identified after control incubation, but not regularly after anti-neurofascin-155 or anti-pan-neurofascin preincubation (see Supplementary Fig. 6). In the control, cell bodies of myelinating Schwann cells were hardly visible. After anti-neurofascin preincubation, on the other hand, Schwann cells bodies appeared more prominent in MAG staining, showing slight neurofascin depositions (see Supplementary Fig. 7). On sensory neurons, anti-pan neurofascin preincubation, but not neurofascin-155 or control serum and IgG preincubation led to an upregulation of NF186 on the sensory neuron membrane (Fig. 5F and Supplementary Fig. 8).

In conclusion, we give *in-vitro* evidence that anti-pan-neurofascin antibodies directly impair paranode formation as well as nodo-paranodal architecture in mature nodes of Ranvier, with more severe effects than anti-neurofascin-155. Furthermore, morphological alterations on myelin and sensory neurons indicate effects of both neurofascin-155 and anti-pan-neurofascin antibodies not only at the node of Ranvier, but other compartments of the peripheral nerve physiologically expressing neurofascin isoforms.

Neurofilament light chain levels as an interindividual disease severity marker

Using the Ella Simple Plex assay, we determined sNF-L levels in seropositive patients and age- and sex-matched healthy controls at first recruitment. In healthy controls, but not in seropositive patients, sNF-L levels correlated to the age ($r = 0.53$, $P = 0.023$). Serum NF-L levels were significantly increased in patients with anti-pan-neurofascin and anti-neurofascin-155 compared to healthy controls (446.7 ± 433.4 versus 70.1 ± 36.2 versus 16.1 ± 6.2 pg/ml, $P < 0.0001$ and $P = 0.0055$). We observed a high variance in sNF-L levels especially in patients with anti-pan-neurofascin. The sNF-L levels in seropositive patients correlated strongly to the disease severity at the nadir, measured by ODSS ($r = 0.80$, $P < 0.001$; see Fig. 6B), GBS-DS ($r = 0.804$, $P < 0.001$) and by MRC sum score ($r = -0.776$, $P < 0.001$). The autoantibody titre at first recruitment neither correlated with the sNF-L levels nor with the clinical scores, but was not determined on treatment-naive patients (see Supplementary Table 1). Due to its long half-life,[42,43] we thus identified sNF-L as a stable interindividual disease severity biomarker, even after initiation of treatment.

Serum NF-L and relative antibody titre for intraindividual follow-up

We assessed serological and clinical parameters at the nadir of disease and long-term follow-up, comparing first-to-last follow-up and including all follow-up data in trend analysis (see Table 2). Aggressive immunomodulatory and immunosuppressive treatment (see above) led to a significant titre decrease in both cohorts, with a median titre from 1:1000 at nadir to 0 at the last follow-up (see Table 2 and Fig. 6). Equally, sNF-L levels decreased in both cohorts during follow-up with a longitudinal downwards trend, but especially in patients with anti-pan-neurofascin (mean ΔsNF-L decrease 498 ± 471 pg/ml in pan-neurofascin versus 31.1 ± 31.4 pg/ml in neurofascin-155, $P = 0.023$). In parallel, clinical scores improved significantly in all patients, especially in patients with anti-pan-neurofascin (mean ΔGBS-DS gain 3 ± 1.2 versus 0.8 ± 1.1 points, $P = 0.015$). We found a strong correlation of sNF-L levels with the clinical scores in the 31 follow-up sera. The relative titre reduction correlated to the relative sNF-L reduction ($r = 0.518$, $P = 0.011$) and also to the relative reduction of clinical scores (see Fig. 6D and Supplementary Fig. 3). Thus, absolute sNF-L levels and relative autoantibody titre were identified as valid follow-up markers for disease activity.

Four patients of the anti-pan-neurofascin cohort initially had highly elevated sNF-L levels (>500 ng/ml). These patients all presented with an acute and severe onset with tetraplegia and need for long-term mechanical ventilation. One of these patients deceased during the acute phase. The others received rituximab, in one case in combination with bortezomib.[27] They showed major motor improvement (ΔMRC 43/48/58) and sNF-L levels < 70 ng/ml in follow-up intervals of 4–11 months, with one of them reaching sNF-L levels within the normal range of healthy controls (3 standard deviations) 9 months after the onset of disease. Supplementary Video 1 shows one of them happily leaving the rehabilitation clinic. Thus, highly elevated sNF-L levels in anti-pan-neurofascin-associated nodo-paranodopathy are reversible. We did not confirm sNF-L as a marker for poor prognosis, but rather as an indicator of acute onset and severe course of disease.

Complement activity *in vivo* associated with titre and sNF-L

Finally, to assess complement activation in our patients not only *in vitro* but also indirectly *in vivo*, we measured patients' serum C3a levels using a commercial ELISA kit. Here, we found no significant differences in absolute C3a levels between controls and patients with anti-pan-neurofascin or neurofascin-155. Still, individual follow-up C3a levels of the patients with anti-pan-neurofascin antibodies who had received IVIg and antibody-depleting therapy followed a linear downwards-trend (ANOVA test for trend: $P = 0.0015$). Furthermore, C3a levels correlated to sNF-L ($r = 0.48$, $P = 0.032$), the absolute titre ($r = 0.66$, $P = 0.002$) and the relative titre ($r = 0.64$, $P = 0.002$) in follow-up sera. Complement activity *in vivo* was thus associated with high antibody titres and acute axonal damage.

Discussion

In this study, we provide evidence of the pathogenicity of anti-pan-neurofascin antibodies including the role of complement in direct comparison to anti-neurofascin-155 associated neuropathy. Furthermore, the longitudinal clinical and serological analysis in a large cohort of patients with anti-pan-neurofascin antibodies indicates a possible favourable outcome despite high morbidity and identifies sNF-L as a marker of the activity of disease.

By detailed longitudinal clinical and serological assessment, we could show that an acute GBS-like onset, severe motor deficits including respiratory failure and prolonged morbidity but monophasic course are unique to anti-pan-neurofascin seropositive patients and in line with previous case studies.[12,20,24,26,27] In contrast to GBS without antibodies, the disease seems to be refractory to standard treatment and the duration of intensive care unit treatment and mechanical ventilation was longer.[44,45] Still, in 8 of 9 cases, antibody production was monophasic without relapse during prolonged follow-up and treatment-free intervals. Further follow-up care for the early identification of a possible relapse remains important for future studies and in clinical routine.

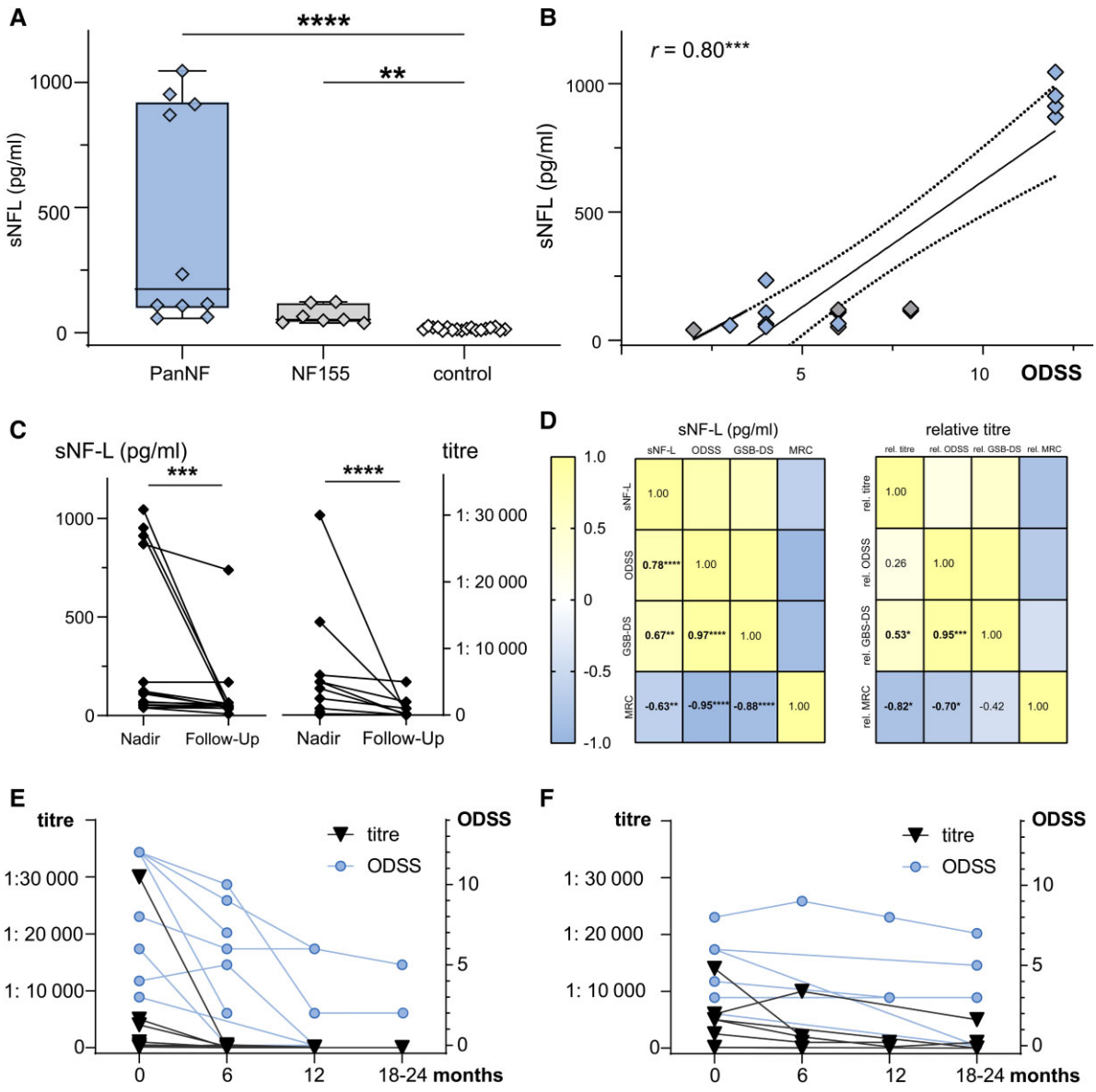

Figure 6 Neurofilament light chain levels, clinical scores and titre including follow-up. (**A**) Serum NF-L levels are shown at the first recruitment in patients with pan-neurofascin (PanNF, blue), neurofascin-155 (NF155, grey) and controls (white) and compared using Kruskal–Wallis test with Dunn's correction for multiple testing. (**B**) The Spearman correlation of sNF-L and the overall disability scale at the first recruitment is shown as scatter dot chart including simple linear regression (line) and 95% confidence intervals (dotted lines), with PanNF-patient marked in blue and neurofascin-155 patients marked in grey. (**C**) Line blots show a significant decrease of sNF-L and the autoantibody titre between the nadir of the disease and the last follow-up, as calculated by Wilcoxon signed rank test. (**D**) Correlation matrices show the correlation of absolute sNF-L with clinical scores in follow-up sera and the correlation of the relative titre reduction with reduction of relative clinical scores in follow-up sera. Numbers show Spearman's coefficient with colour coding as indicated in the legend. Significant correlations are highlighted in bold letters and by asterisk. (**E** and **F**) Absolute antibody titres and ODSS are shown at follow-up intervals between 0 and 24 months in patients with anti-PanNF (**E**) and NF155 antibodies (**F**). In contrast to NF155, antibody titres decrease completely in PanNF-associated disease. Significance level: $^{*}P < 0.05$, $^{**}P < 0.01$, $^{***}P < 0.001$, $^{****}P < 0.00001$.

In chronic autoimmune neuropathy pan-neurofascin does not seem to be a common target.[46] Chronic disease was characteristic for anti-neurofascin-155 seropositive patients, who presented with characteristics as previously described, such as a young onset, ataxia and tremor, and a good outcome under immunosuppressive therapy.[9,11,12,47]

In contrast to previous reports on anti-pan-neurofascin, which were mostly limited to clinical data, subclass and epitope analysis, our experimental data support a relationship between the severe phenotype and the pathogenic effects of autoantibodies on nodes of Ranvier. We show that anti-pan-neurofascin antibodies access and damage the nodal region directly, whereas anti-neurofascin-155 antibodies merely reach their paranodal target in living neurons. Our data are in line with a recent study that could demonstrate nodal binding of anti-pan-neurofascin sera on myelinated human stem cell-derived sensory neurons. We now provide additional insights by performing co-staining with a commercial anti-pan-neurofascin antibody, and could clearly show that low paranodal binding is not caused by immediate neurofascin-155 degradation or diffusion, but in fact by a low accessibility to the paranode that is protected by the terminal myelin loops and thus less exposed than nodal neurofascin-186.[19,48] This direct access of anti-pan-neurofascin

Table 2 Clinical and serological follow-up parameters in seropositive patients

Cohort and parameter	Nadir	Last follow-up	P-value (Wilcoxon)	P-value (test for trend)
Whole cohort				
Titre	1:1000 (1:100–1:30 000)	0 (0–1:5000)	<0.0001	<0.0001
NF-L (pg/ml)	115 (39–1045)	46.6 (8.7–738)	0.0002	0.0242
ODSS	6 (2–12)	3 (0–12)	0.0010	0.0004
MRC	47.5 (0–60)	50.50 (0–60)	0.0254	0.688
GBS-DS	3 (1–4)	2 (0–6)	0.0049	0.0030
Mean C3a (ng/ml)	1.87 ± 1.14	0.46 ± 0.17	0.030	0.0297
Pan-neurofascin subcohort				
Titre	1:500 (1:100–1:30 000)	0 (0–1:200)	0.0078	<0.0001
NF-L (pg/ml)	870 (70.2–1045)	50 (31.7–748)	0.0313	<0.0001
ODSS	9 (3–12)	4 (0–12)	0.0313	0.001
MRC	36 (0–60)	45.5 (0–60)	0.093	0.681
GBS-DS	4 (1–5)	2 (0–6)	0.023	0.0030
Mean C3a (ng/ml)	2.12 ± 1.09	0.45 ± 0.20	0.0302	0.0052
Neurofascin-155 subcohort				
Titre	1:5000 (1:100–1:14 000)	1:1000 (0–1:5000)	0.0156	0.0085
NF-L (pg/ml)	54 (39–123)	39.2 (8.7–60.7)	0.0156	0.0546
ODSS	6 (2–6)	3 (0–7)	0.0625	0.0058
MRC	51 (46–56)	55.5 (50–60)	0.125	0.060
GBS-DS	3 (1–3)	2 (0–3)	0.250	0.033

Median values including the range in brackets or mean value ± standard deviation at the clinical nadir of disease and at the last follow-up time point are shown for the whole cohort, for the anti-pan-neurofascin subcohort and for the anti-neurofascin-155 subcohort. Results of statistical testing comparing the two time points are shown in column four (Wilcoxon signed rank test. C3a levels were compared using paired *t*-test). We not only included statistical comparison of the nadir-to-last value, but also included an analysis for linear trend considering all single follow-up intervals and values using ANOVA test for linear trends, as shown in the last column.

antibodies to nodal targets in comparison to anti-neurofascin-155 could contribute to the acute and more severe phenotype of pan-neurofascin-associated disease. However, the binding strongly depended on the autoantibody titre. A correlation of clinical disease severity and titre in neurofascin-155 associated paranodopathy has been reported.[49] We conclude that the clinical disease severity is directly linked to the titre.

Furthermore, we observed binding of anti-neurofascin-155 to the myelinating Schwann cell surface. Previous *in vitro* and *in vivo* studies have reported binding to surface antigens of Schwann cells around paranodes in neonatal rats and on cultured oligodendrocytes, proposing effects on paranodal myelin turnover and paranode formation.[11,19] Here, we observe binding not only at paranodal microvilli, but along the whole myelinating Schwann cell including the outer mesaxon and the Schwann cell body, as most recently also described for bivalent neurofascin-155 IgG antibodies, which cluster neurofascin-155 at these locations and lead to paranodal neurofascin depletion.[50] Still, both previous studies as well as our study have observed these effects in embryonic or neonatal rodent models.[19,50] Future studies need to address the effect of anti-neurofascin antibodies on myelinating Schwann cells including cell metabolism and protein expression in human cell culture models and adult *in vivo* models.

In vitro qualitative analysis and additional high content morphometrical analysis of myelinating co-cultures using advanced imaging techniques allowed us to pinpoint anti-pan-neurofascin-related pathogenicity. We report an impact of anti-neurofascin antibodies on nodo-paranodal architecture both during myelination and on already formed nodes and paranodes. Paranode formation depends on the integrity of the junctional axoglial contact,[51,52] being disturbed by anti-neurofascin-155 binding.[19] Our data confirm impairment of paranode formation in anti-neurofascin-155 during myelination, but more importantly, show even more severe impairment after pan-neurofascin preincubation. The nodal isoform neurofascin-186 is essential for the organization of intact peripheral nodes of Ranvier.[53–55] Neurofascin-186 could contribute to intact paranode formation, as a pan-neurofascin knockout reportedly leads to a dispersion and absence of Caspr-1, with more severe effects on nerve conduction in case of double knockout.[55,56] Anti-pan-neurofascin antibodies possibly impair clustering of nodo-paranodal proteins more severely by binding to all neurofascin isoforms including embryonic neurofascin-140.[33]

Furthermore, we provide evidence that anti-pan-neurofascin antibodies lead to a severe paranodal neurofascin degradation in more mature nodes. A previous study suggested that anti-neurofascin-155 does not have the capacity to affect its target if firmly stabilized at the paranode.[19] In our study, anti-neurofascin-155 preincubation led to a loss of paranodal neurofascin, albeit to a much lower degree than anti-pan-neurofascin. Antibody-induced nodo-paranodal degradation of neurofascins and impairment of the paranodal junction most probably are followed by alterations to the nodal gap, as observed in our co-cultures and previously described in both neurofascin and Caspr-1 knockout models.[55–59] Additionally, we observed effects on paranodal myelination such as paranodal swelling and formation of myelin balls. Paranodal swelling and myelin alterations have been reported in antibody-mediated demyelinating neuropathy including paranodopathy.[18,47,60–62] In contrast to a previous report of anti-pan-neurofascin-associated nodo-paranodoapthy,[22] where *in vivo* histopathological changes were restricted to the nodal region, we now report a complex pathology not only affecting the nodal region, but also the paranodal junction, paranodal myelination, neurofascin clustering along the myelinated axon, Schmidt Lantermann incisure formation and even sensory neuron membrane protein expression in pan-neurofascin-associated disease. This highly impaired nodo-paranodal and cell-associated pathology most probably contributes to the more severe clinical

phenotype of anti-pan-neurofascin-associated neuropathy compared to anti-neurofascin-155.

Surprisingly, we observed neurofascin-186 enrichment at the sensory neuron membrane after long-term anti-pan-neurofascin IgG3/IgG4 preincubation. Previously, we showed that anti-contactin-1 IgG4 antibodies had quite the opposing effect: contactin-1, which is physiologically expressed at neuronal cell membranes including the DRG,[63,64] was significantly decreased, affecting sodium currents.[34] Neuronal neurofascin-186, however, is not enriched at the DRG membrane under physiological conditions, but restricted to the node of Ranvier in the PNS.[65–67] Ectopic neurofascin-186 overexpression has been shown to have pathological effects including the clustering of extracellular matrix protein located around sensory cells.[66] Whether neurofascin-186 clustering at the sensory neuron membrane occurs due to IgG3-related cross-linking[28,29] and aggregation or due to upregulation of neurofascin-186 must be investigated in further studies. A recent study showed that despite IgG4 subclass, neurofascin-155-related pathogenicity depends on monospecific and bivalent antibodies, which can potentially induce cross-linking and internalization, similarly to IgG3.[50] The consecutive effects of neurofascin-186 membrane clustering on a molecular and a clinical level, including IgG subclass and valency-related effects, should be addressed in the future. Furthermore, *in vivo* studies are needed to assess functional and electrophysiological effects of anti-pan-neurofascin.

Besides differences in the accessibility of the target autoantigen, different IgG subclasses may account for disparate clinical phenotypes: whereas anti-neurofascin-155 autoantibodies mostly belong to the IgG4 subclass, concurrent IgG3 and IgG4 autoantibodies could be detected in anti-pan-neurofascin patients. Previous studies reported IgG3-dependent complement binding in nodo-paranodopathy.[12,20,30,68] IgG3 has a long, semi-rigid hinge region that favours binding to FcγR and C1q binding and makes it the strongest complement activator of all IgG subclasses.[69,70] Here, we quantitatively assessed not only binding, but also effector functions and found increased complement activity associated to IgG3 subclass, leading to an increased cytotoxicity. As a possible clinical *in vivo* correlate, serum C3a levels correlated to the antibody titre and indirect signs of axonal damage during follow-up.

Here, we show that IVIg inhibits autoantibody-dependent complement deposition and cytotoxicity *in vitro*. The effect of IVIg on antibody-mediated effector functions rather than antibody binding is in line with previous studies investigating the effect of IVIg in antibody-mediated disease.[30,71–73] However, IVIg response was only temporal and not sufficient in patients with anti-pan-neurofascin IgG3/4 of our cohort, similar to previous studies including patients with autoimmune nodopathies.[12,20,22] The potency of IVIg could be limited in fulminant disease due to high-titre antibody production. Furthermore, using *in vitro* preincubation experiments, we could show that anti-neurofascin-155 and anti-pan-neurofascin antibodies are directly pathogenic, in absence of humoral complement factors. Still, nodo-paranodal destruction might be aggravated in presence of complement, as we observed more severe morphological alterations when using serum possibly containing complement factors compared to purified IgG. This indicates that complement-mediated mechanisms might only play an additional role on top of effects induced by direct pathogenicity. Furthermore, subclass switching from IgG3 to IgG4 from the acute to chronic stage, as previously reported in anti-contactin-associated nodo-paranodopathy, might play a role.[6] Due to late recruitment in most patients, we could not study subclass switch at onset and detected simultaneous presence of IgG3 and IgG4 in our patients. In conclusion, pathology includes most probably direct, complement-independent mechanisms as well as additional IgG3-associated complement-mediated damage in the acute phase.[74] IVIg might thus only be considered as a complementary therapy to antibody-depleting treatment options in IgG1/3-related disease.

As in previous studies including patients with IgG-related autoimmune nodopathy,[10,13,49,68,75,76] our anti-neurofascin cohort shows a good response to antibody depleting therapy with rituximab. Still, rituximab dosage and intervals were heterogeneous, as in previously reported studies,[49] and several different treatments were applied. As there are still no common guidelines available on rituximab schemes for autoimmune nodopathy and clinical trials including dosing schemes are still ongoing,[14,77] further studies are urgently needed to investigate optimal dosage and intervals of rituximab and efficacy of further treatment regimen in a standardized manner.

Although patients with IgG3/4 respond well to rituximab, IgG1-associated disease, which has been previously reported in a cohort of anti-pan-neurofascin patients,[26] seems to be more refractory to rituximab treatment,[78] possibly explaining a poorer outcome in that study compared to ours. Still, the phenotype of these anti-pan-neurofascin IgG1 seropositive patients resembled the phenotype of anti-pan-neurofascin IgG3 patients described here and in previous studies.[12,20,21] These differences in the subclass profile could either occur due to slight interlaboratory differences in subclass testing,[79] or could be cohort-related. Interlaboratory validation of subclass screening should be further investigated, as subclass assessment could be decisive for individual treatment options in these rare but severely affected patients.

As an outlook, the safety and efficacy of more potent complement-directed therapy options including eculizumab and next-generation complement drugs[80] could be investigated both *in vitro* and *in vivo* in patients with IgG1/3. The C5 inhibitor eculizumab successfully and safely reduces complement-mediated pathology in IgG1/3 acetylcholine receptor antibody seropositive myasthenia gravis with higher efficacy than IVIg.[81–83] However, only small studies and case series are available in acute immune-mediated neuropathy, indicating a positive trend towards efficacy.[84–87] Our study provides *in vitro* and *in vivo* evidence of complement-related pathology in anti-pan-neurofascin-associated nodo-paranodopathy and thus sets the basis for further studies considering new therapeutic options in these severely affected individuals.

In this study, we identify sNF-L levels as a possible marker for interindividual disease severity and intraindividual follow-up. As proposed before, anti-pan-neurofascin patients do not fit into classical categories of autoimmune demyelinating neuropathy and biomarkers of peripheral nerve injury might be of greater efficacy for treatment decisions than the mere diagnosis.[26] Here, we can show that sNF-L is highly elevated in pan-neurofascin seropositive patients compared to neurofascin-155 and healthy controls. As described in multiple sclerosis, vasculitic neuropathy and GBS,[88–92] we found sNF-L to be a marker especially for acute disease and a surrogate parameter for clinical disease severity. We failed to detect a correlation of sNF-L to the titres at first recruitment, as previously described in baseline sera of anti-neurofascin-155-associated disease,[49] probably because our patients were not treatment-naive with possible influence on the antibody titre (see Supplementary Fig. 3). Relative autoantibody titres during follow-up correlated with sNF-L and clinical scores, qualifying both serum titre and sNF-L as a valid longitudinal biomarker during follow-up and as possible sensitive indicators of a need of therapy escalation, especially if evaluation during critical care treatment is limited. At testing, one should consider the different kinetics of both biomarkers:

the long half-life of sNF-L,[42,43] but the immediate titre response to treatment.[10,68,76] Together, both biomarkers allow precise monitoring and precision care during follow-up.

Here, despite highly elevated sNF-L in the acute phase, the ability to walk was recovered in our severely affected patients. Still, despite clinically and serologically monophasic disease, sNF-L levels only reached normal levels in one patient with anti-pan-neurofascin antibodies, considering the long half-life probably due to short follow-up intervals of 4–11 months assessing sNF-L. Previous study reported sNF-L as an indicator for poor prognosis in inflammatory neuropathies.[90,93,94] Of importance, our data indicate that highly elevated sNF-L should not necessarily be considered a marker of poor prognosis in autoantibody-mediated acute nodo-paranodopathy, but as a marker for fulminant course including critical care treatment and the need for intensive immunomodulatory treatment, with the possibility of recovery. This finding is in line with previous reports on elevated NF-L in acute and severe GBS, independent of primary axonal or demyelinating neuropathy.[91,92]

Despite the high morbidity and months of intensive care unit treatment, our serological and clinical data show that anti-pan-neurofascin seropositive survivors can have a favourable outcome. Similar to other autoantibody-mediated, fulminant neurological diseases requiring long-term critical care treatment,[95] recovery is possible and should thus motivate physicians to not discuss therapy limitations too early. In GBS, especially in patients with fulminant course, failure of standard treatment and highly elevated sNF-L, early antibody screening should be considered. With the notion of direct pathogenicity of the antibodies, early and aggressive immunomodulatory treatment may improve outcome, as also reported in antibody-mediated encephalitis.[95] A limitation to our study is that treatment was heterogeneous in our cohort, and we cannot conclude if monophasic course was endogenous or induced by treatment regimen. Still, as remission can occur in anti-pan-neurofascin-associated disease and, rarely, also in neurofascin-155-associated disease,[49] further treatment might not be necessary after initial antibody depletion in some cases. Our data thus support a 'watchful-waiting' strategy in case of clinical improvement in combination with the complete absence of antibodies and an sNF-L decrease.

In conclusion, our study provides evidence for the pathogenicity of pan-neurofascin antibodies including complement-mediated pathways and raises awareness that its associated distinct clinical phenotype is of high relevance during the diagnostic work-up and treatment of acute and severe immune-mediated neuropathy.

Acknowledgements

We thank Barbara Reuter, Antonia Kohl, Sonja Mildner and Hiltrud Klüpfel for excellent technical assistance. We thank Heike Rittner and Nadine Cebulla for providing sNF-L data of a cohort of healthy controls. The authors especially thank the patients and animals who contributed to the study.

Funding

No specific funding was received towards this work. L.A. and K.D. are supported by research fellowships by the Interdisciplinary Center of Clinical Research of the Medical Faculty of Würzburg ("Interdisziplinäres Zentrum für Klinische Forschung, Universitätsklinikum Würzburg", IZKF). K.D. is supported by a grant of the German Research Foundation (Deutsche Forschungsgemeinschaft, DFG, Grant number DO-2219/1-1). K.D. and K.G.H. are supported by a grant of the IZKF (see above; Grant number F-N-439). J.M. and J.L. hold medical doctoral researchers' fellowships (MD Excellence Program) of the Graduate School of Life Sciences, Julius-Maximilians-Universität Würzburg.

Competing interests

L.A., F.L., C.S. and K.D. work for an academic institution offering commercial antibody diagnostics. I.A. has received travel grants from Biogen Idec and Guthy-Jackson Charitable Foundation, served on scientific advisory boards for Roche, Alexion, Merck and received research support from Diamed, none related to this manuscript. A.L.F. received research funding from Georgius Agricola Stiftung Ruhr, Ruhr University Bochum (FoRUM-program) and GBS CIDP Foundation International. She owns shares of Fresenius SE & Co., Gilead Sciences, Medtronic PLC and Novartis AG. F.L. serves or has served on advisory boards for Biogen, Roche and Alexion and received speaker honoraria from Roche, Biogen, Grifols, Alexion, Desitin and Novartis. He serves as editorial board member for Neurology N2. J.M. received travel grants from Biogen idec. His research is funded by Klaus Tschira Foundation, Hertie Foundation, Novartis, Biogen and Ruhr-University, Bochum (FoRUM-Program), none related to this work. K.P. received travel grants and speaker honoraria from Biogen Idec and Bayer Schering, Novartis, Celgene and Grifols and has participated in advisory board meeting for Celgene, none related to this manuscript. C.S. has served on scientific advisory boards for Akcea, Algiax, Air Liquide, Bayer, Grifols, Ipsen, LFB, Immunic, Merz, Pfizer, Roche and Takeda. She received speaker honoraria from Akcea, Alnylam Amicus, Grifols, Pfizer and Teva. She serves or has served as a journal editor, associate editor or editorial advisory board member for the *European Journal of Neurology*, *PLoS One* and *PAIN Reports*. The other authors report no competing interests.

Supplementary material

Supplementary material is available at *Brain* online.

References

1. van den Berg B, Walgaard C, Drenthen J, Fokke C, Jacobs BC, van Doorn PA. Guillain–Barré syndrome: Pathogenesis, diagnosis, treatment and prognosis. *Nat Rev Neurol*. 2014;10:469-482.
2. Leonhard SE, Mandarakas MR, Gondim FAA, *et al*. Diagnosis and management of Guillain–Barré syndrome in ten steps. *Nat Rev Neurol*. 2019;15:671-683.
3. Ng JK, Malotka J, Kawakami N, *et al*. Neurofascin as a target for autoantibodies in peripheral neuropathies. *Neurology*. 2012;79:2241-2248.
4. Devaux JJ, Odaka M, Yuki N. Nodal proteins are target antigens in Guillain–Barré syndrome. *J Peripher Nerv Syst*. 2012;17:62-71.
5. Miura Y, Shahrizaila N, Yuki N. Biomarkers of 'acute-onset' chronic inflammatory demyelinating polyneuropathy. *Brain*. 2015;138(Pt 3):e335.
6. Appeltshauser L, Brunder AM, Heinius A, *et al*. Antiparanodal antibodies and IgG subclasses in acute autoimmune neuropathy. *Neurol Neuroimmunol Neuroinflamm*. 2020;7:e817.
7. Pascual-Goñi E, Fehmi J, Lleixà C, *et al*. Antibodies to the Caspr1/contactin-1 complex in chronic inflammatory demyelinating polyradiculoneuropathy. *Brain*. 2021;144:1183-1196.

8. Querol L, Nogales-Gadea G, Rojas-Garcia R, *et al*. Antibodies to contactin-1 in chronic inflammatory demyelinating polyneuropathy. *Ann Neurol*. 2013;73:370-380.
9. Querol L, Nogales-Gadea G, Rojas-Garcia R, *et al*. Neurofascin IgG4 antibodies in CIDP associate with disabling tremor and poor response to IVIg. *Neurology*. 2014;82:879-886.
10. Doppler K, Appeltshauser L, Wilhelmi K, *et al*. Destruction of paranodal architecture in inflammatory neuropathy with anti-contactin-1 autoantibodies. *J Neurol Neurosurg Psychiatry*. 2015;86:720-728.
11. Devaux JJ, Miura Y, Fukami Y, *et al*. Neurofascin-155 IgG4 in chronic inflammatory demyelinating polyneuropathy. *Neurology*. 2016;86:800-807.
12. Delmont E, Manso C, Querol L, *et al*. Autoantibodies to nodal isoforms of neurofascin in chronic inflammatory demyelinating polyneuropathy. *Brain*. 2017;140:1851-1858.
13. Dalakas MC. IgG4-mediated neurologic autoimmunities. Understanding the pathogenicity of IgG4, ineffectiveness of IVIg, and long-lasting benefits of anti–B cell therapies. *Neurol Neuroimmunol Neuroinflamm*. 2022;9:e1116.
14. Van den Bergh PYK, van Doorn PA, Hadden RDM, *et al*. European Academy of Neurology/Peripheral Nerve Society guideline on diagnosis and treatment of chronic inflammatory demyelinating polyradiculoneuropathy: Report of a joint task force—Second revision. *J Peripher Nerv Syst*. 2021;26:242-268.
15. Uncini A, Mathis S, Vallat JM. New classification of autoimmune neuropathies based on target antigens and involved domains of myelinated fibres. *J Neurol Neurosurg Psychiatry*. 2022;93:57-67.
16. Labasque M, Hivert B, Nogales-Gadea G, Querol L, Illa I, Faivre-Sarrailh C. Specific contactin N-glycans are implicated in neurofascin binding and autoimmune targeting in peripheral neuropathies. *J Biol Chem*. 2014;289:7907-7918.
17. Manso C, Querol L, Mekaouche M, Illa I, Devaux JJ. Contactin-1 IgG4 antibodies cause paranode dismantling and conduction defects. *Brain*. 2016;139(Pt 6):1700-1712.
18. Koike H, Kadoya M, Kaida KI, *et al*. Paranodal dissection in chronic inflammatory demyelinating polyneuropathy with anti-neurofascin-155 and anti-contactin-1 antibodies. *J Neurol Neurosurg Psychiatry*. 2017;88:465-473.
19. Manso C, Querol L, Lleixa C, *et al*. Anti-neurofascin-155 IgG4 antibodies prevent paranodal complex formation *in vivo*. *J Clin Invest*. 2019;129:2222-2236.
20. Stengel H, Vural A, Brunder AM, *et al*. Anti-pan-neurofascin IgG3 as a marker of fulminant autoimmune neuropathy. *Neurol Neuroimmunol Neuroinflamm*. 2019;6:e603.
21. Burnor E, Yang L, Zhou H, *et al*. Neurofascin antibodies in autoimmune, genetic, and idiopathic neuropathies. *Neurology*. 2018;90:e31-e38.
22. Vallat JM, Mathis S, Magy L, *et al*. Subacute nodopathy with conduction blocks and anti-neurofascin 140/186 antibodies: An ultrastructural study. *Brain*. 2018;141:e56.
23. Rempe T, Ho KWD, Shahid M, Yang LJ, Chuquilin M. Neurofascin-140 and -155 antibodies in an atypical case of POEMS syndrome. *Muscle Nerve*. 2019;60:E1-e3.
24. De Simoni D, Ricken G, Winklehner M, *et al*. Antibodies to nodal/paranodal proteins in paediatric immune-mediated neuropathy. *Neurol Neuroimmunol Neuroinflamm*. 2020;7:e763.
25. Li V, Schon F, Fehmi J, Modarres H, Rinaldi S, Rossor AM. Motor neuropathy with conduction block due to pan-neurofascin antibodies in a patient with chronic lymphocytic leukemia. *Muscle Nerve*. 2020;61:E41-e44.
26. Fehmi J, Davies AJ, Walters J, *et al*. IgG(1) pan-neurofascin antibodies identify a severe yet treatable neuropathy with a high mortality. *J Neurol Neurosurg Psychiatry*. 2021;92:1089-1095.
27. Fels M, Fisse AL, Schwake C, *et al*. Report of a fulminant anti-pan-neurofascin-associated neuropathy responsive to rituximab and bortezomib. *J Peripher Nerv Syst*. 2021;26:475-480.
28. Bruhns P, Iannascoli B, England P, *et al*. Specificity and affinity of human fcgamma receptors and their polymorphic variants for human IgG subclasses. *Blood*. 2009;113:3716-3725.
29. Kapur R, Einarsdottir HK, Vidarsson G. IgG-effector functions: "The good, the bad and the ugly". *Immunol Lett*. 2014;160:139-144.
30. Appeltshauser L, Weishaupt A, Sommer C, Doppler K. Complement deposition induced by binding of anti-contactin-1 auto-antibodies is modified by immunoglobulins. *Exp Neurol*. 2017;287(Pt 1):84-90.
31. Doppler K, Appeltshauser L, Kramer HH, *et al*. Contactin-1 and neurofascin-155/-186 are not targets of auto-antibodies in multifocal motor neuropathy. *PLoS One*. 2015;10:e0134274.
32. Moritz CP, Tholance Y, Lassabliere F, Camdessanche JP, Antoine JC. Reducing the risk of misdiagnosis of indirect ELISA by normalizing serum-specific background noise: The example of detecting anti-FGFR3 autoantibodies. *J Immunol Methods*. 2019;466:52-56.
33. Zhang A, Desmazieres A, Zonta B, *et al*. Neurofascin 140 is an embryonic neuronal neurofascin isoform that promotes the assembly of the node of Ranvier. *J Neurosci*. 2015;35:2246-2254.
34. Grüner J, Stengel H, Werner C, *et al*. Anti–contactin-1 antibodies affect surface expression and sodium currents in dorsal root ganglia. *Neurol Neuroimmunol Neuroinflamm*. 2021;8:e1056.
35. Gauthier A, Viel S, Perret M, *et al*. Comparison of Simoa™ and Ella™ to assess serum neurofilament-light chain in multiple sclerosis. *Ann Clin Transl Neurol*. 2021;8:1141-1150.
36. Aldo P, Marusov G, Svancara D, David J, Mor G. Simple Plex(™) : A novel multi-analyte, automated microfluidic immunoassay platform for the detection of human and mouse cytokines and chemokines. *Am J Reprod Immunol*. 2016;75:678-693.
37. Taveggia C, Bolino A. DRG neuron/Schwann cells myelinating cocultures. *Methods Mol Biol*. 2018;1791:115-129.
38. Stettner M, Wolffram K, Mausberg AK, *et al*. A reliable *in vitro* model for studying peripheral nerve myelination in mouse. *J Neurosci Methods*. 2013;214:69-79.
39. Kleyweg RP, van der Meche FG, Schmitz PI. Interobserver agreement in the assessment of muscle strength and functional abilities in Guillain–Barré syndrome. *Muscle Nerve*. 1991;14:1103-1109.
40. Merkies IS, Schmitz PI, van der Meche FG, Samijn JP, van Doorn PA. Clinimetric evaluation of a new overall disability scale in immune mediated polyneuropathies. *J Neurol Neurosurg Psychiatr*. 2002;72:596-601.
41. Hughes RA, Newsom-Davis JM, Perkin GD, Pierce JM. Controlled trial prednisolone in acute polyneuropathy. *Lancet*. 1978;312:750-753.
42. Thebault S, Booth RA, Freedman MS. Blood neurofilament light chain: The neurologist's troponin? *Biomedicines*. 2020;8:523.
43. Verde F, Otto M, Silani V. Neurofilament light chain as biomarker for amyotrophic lateral sclerosis and frontotemporal dementia. *Front Neurosci*. 2021;15:679199.
44. Netto AB, Taly AB, Kulkarni GB, Uma Maheshwara Rao GS, Rao S. Complications in mechanically ventilated patients of Guillain–Barré syndrome and their prognostic value. *J Neurosci Rural Pract*. 2017;8:68-73.
45. Shang P, Feng J, Wu W, Zhang HL. Intensive care and treatment of severe Guillain–Barré syndrome. *Front Pharmacol*. 2021;12:608130.
46. Delmont E, Brodovitch A, Kouton L, *et al*. Antibodies against the node of Ranvier: A real-life evaluation of incidence, clinical features and response to treatment based on a prospective analysis of 1500 sera. *J Neurol*. 2020;267:3664-3672.

47. Shelly S, Klein CJ, Dyck PJB, *et al*. Neurofascin-155 immunoglobulin subtypes: Clinicopathologic associations and neurologic outcomes. *Neurology*. 2021;97:e2392-e2403.
48. Gao Y, Kong L, Liu S, Liu K, Zhu J. Impact of neurofascin on chronic inflammatory demyelinating polyneuropathy via changing the node of Ranvier function: A review. *Front Mol Neurosci*. 2021;14:779385.
49. Martín-Aguilar L, Lleixà C, Pascual-Goñi E, *et al*. Clinical and laboratory features in anti-NF155 autoimmune nodopathy. *Neurol Neuroimmunol Neuroinflamm*. 2022;9:e1098.
50. Jentzer A, Attal A, Roué C, *et al*. IgG4 valency modulates the pathogenicity of anti-neurofascin-155 IgG4 in autoimmune nodopathy. *Neurol Neuroimmunol Neuroinflamm*. 2022;9: e200014.
51. Pedraza L, Huang JK, Colman D. Disposition of axonal caspr with respect to glial cell membranes: Implications for the process of myelination. *J Neurosci Res*. 2009;87:3480-3491.
52. Eisenbach M, Kartvelishvily E, Eshed-Eisenbach Y, *et al*. Differential clustering of caspr by oligodendrocytes and Schwann cells. *J Neurosci Res*. 2009;87:3492-3501.
53. Labasque M, Devaux JJ, Lévêque C, Faivre-Sarrailh C. Fibronectin type III-like domains of neurofascin-186 protein mediate gliomedin binding and its clustering at the developing nodes of Ranvier. *J Biol Chem*. 2011;286:42426-42434.
54. Amor V, Zhang C, Vainshtein A, *et al*. The paranodal cytoskeleton clusters Na^+ channels at nodes of Ranvier. *Elife*. 2017;6: e21392.
55. Sherman DL, Tait S, Melrose S, *et al*. Neurofascins are required to establish axonal domains for saltatory conduction. *Neuron*. 2005;48:737-742.
56. Taylor AM, Saifetiarova J, Bhat MA. Postnatal loss of neuronal and glial neurofascins differentially affects node of Ranvier maintenance and myelinated axon function. *Front Cell Neurosci*. 2017;11:11.
57. Zhang Y, Yuen S, Peles E, Salzer JL. Accumulation of neurofascin at nodes of Ranvier is regulated by a paranodal switch. *J Neurosci*. 2020;40:5709-5723.
58. Pillai AM, Thaxton C, Pribisko AL, Cheng JG, Dupree JL, Bhat MA. Spatiotemporal ablation of myelinating glia-specific neurofascin (Nfasc NF155) in mice reveals gradual loss of paranodal axoglial junctions and concomitant disorganization of axonal domains. *J Neurosci Res*. 2009;87:1773-1793.
59. Thaxton C, Pillai AM, Pribisko AL, *et al*. *In vivo* deletion of immunoglobulin domains 5 and 6 in neurofascin (Nfasc) reveals domain-specific requirements in myelinated axons. *J Neurosci*. 2010;30:4868-4876.
60. Cai Z, Finnie JW, Blumbergs PC, Manavis J, Ghabriel MN, Thompson PD. Early paranodal myelin swellings (tomacula) in an avian riboflavin deficiency model of demyelinating neuropathy. *Exp Neurol*. 2006;198:65-71.
61. Kawagashira Y, Koike H, Tomita M, *et al*. Morphological progression of myelin abnormalities in IgM-monoclonal gammopathy of undetermined significance anti-myelin-associated glycoprotein neuropathy. *J Neuropathol Exp Neurol*. 2010;69:1143-1157.
62. Cai Z, Blumbergs PC, Koblar SA, *et al*. Peripheral nervous system and central nervous system pathology in rapidly progressive lower motor neuron syndrome with immunoglobulin M anti-GM1 ganglioside antibody. *J Peripher Nerv Syst*. 2004;9:79-91.
63. Tan RPA, Leshchyns'ka I, Sytnyk V. Glycosylphosphati dylinositol-anchored immunoglobulin superfamily cell adhesion molecules and their role in neuronal development and synapse regulation. *Front Mol Neurosci*. 2017;10:378.
64. Treubert U, Brümmendorf T. Functional cooperation of beta1-integrins and members of the Ig superfamily in neurite outgrowth induction. *J Neurosci*. 1998;18:1795-1805.
65. Alpizar SA, Baker AL, Gulledge AT, Hoppa MB. Loss of neurofascin-186 disrupts alignment of AnkyrinG relative to its binding partners in the axon initial segment. *Front Cell Neurosci*. 2019;13:1.
66. Hedstrom KL, Xu X, Ogawa Y, *et al*. Neurofascin assembles a specialized extracellular matrix at the axon initial segment. *J Cell Biol*. 2007;178:875-886.
67. Abouelezz A, Hotulainen P. NuMA1 facilitates the assembly of the axon initial segment by promoting the retention of neurofascin-186. *J Cell Biol*. 2020;219:e201911139.
68. Doppler K, Appeltshauser L, Villmann C, *et al*. Auto-antibodies to contactin-associated protein 1 (caspr) in two patients with painful inflammatory neuropathy. *Brain*. 2016;139(Pt 10):2617-2630.
69. Vidarsson G, Dekkers G, Rispens T. IgG subclasses and allotypes: From structure to effector functions. *Front Immunol*. 2014;5:520.
70. Spiteri VA, Goodall M, Doutch J, Rambo RP, Gor J, Perkins SJ. Solution structures of human myeloma IgG3 antibody reveal extended Fab and Fc regions relative to the other IgG subclasses. *J Biol Chem*. 2021;297:100995.
71. Basta M, Dalakas MC. High-dose intravenous immunoglobulin exerts its beneficial effect in patients with dermatomyositis by blocking endomysial deposition of activated complement fragments. *J Clin Invest*. 1994;94:1729-1735.
72. Dalakas MC. Mechanistic effects of IVIg in neuroinflammatory diseases: Conclusions based on clinicopathologic correlations. *J Clin Immunol*. 2014;34(Suppl 1):120-126.
73. Latov N. Immune mechanisms, the role of complement, and related therapies in autoimmune neuropathies. *Expert Rev Clin Immunol*. 2021;17:1269-1281.
74. Dalakas MC. Autoimmune neurological disorders with IgG4 antibodies: A distinct disease spectrum with unique IgG4 functions responding to anti-B cell therapies. *Neurotherapeutics*. 2022;19:741–752.
75. Koneczny I, Tzartos J, Mané-Damas M, *et al*. IgG4 autoantibodies in organ-specific autoimmunopathies: Reviewing class switching, antibody-producing cells, and specific immunotherapies. *Front Immunol*. 2022;13:834342.
76. Querol L, Rojas-Garcia R, Diaz-Manera J, *et al*. Rituximab in treatment-resistant CIDP with antibodies against paranodal proteins. *Neurol Neuroimmunol Neuroinflamm*. 2015;2:e149.
77. Shimizu S, Iijima M, Fukami Y, *et al*. Efficacy and safety of rituximab in refractory CIDP with or without IgG4 autoantibodies (RECIPE): Protocol for a double-blind, randomized, placebo-controlled clinical trial. *JMIR Res Protoc*. 2020;9:e17117.
78. Zografou C, Vakrakou AG, Stathopoulos P. Short- and long-lived autoantibody-secreting cells in autoimmune neurological disorders. *Front Immunol*. 2021;12:686466.
79. Rinaldi S. Inter-laboratory validation of nodal/paranodal antibody testing. PNS 2022 Annual Meeting eLibrary. 2022;356942:1384.
80. Mastellos DC, Ricklin D, Lambris JD. Clinical promise of next-generation complement therapeutics. *Nat Rev Drug Discov*. 2019;18:707-729.
81. Howard JF J, Utsugisawa K, Benatar M, *et al*. Safety and efficacy of eculizumab in anti-acetylcholine receptor antibody-positive refractory generalised myasthenia gravis (REGAIN): A phase 3, randomised, double-blind, placebo-controlled, multicentre study. *Lancet Neurol*. 2017;16:976-986.
82. Muppidi S, Utsugisawa K, Benatar M, *et al*. Long-term safety and efficacy of eculizumab in generalized myasthenia gravis. *Muscle Nerve*. 2019;60:14-24.
83. Jacob S, Murai H, Utsugisawa K, *et al*. Response to eculizumab in patients with myasthenia gravis recently treated with chronic IVIg: a subgroup analysis of REGAIN and its open-label extension study. *Ther Adv Neurol Disord*. 2020;13: 1756286420911784.

84. Misawa S, Kuwabara S, Sato Y, *et al*. Safety and efficacy of eculizumab in Guillain–Barré syndrome: A multicentre, double-blind, randomised phase 2 trial. *Lancet Neurol*. 2018;17:519-529.
85. Querol LA, Hartung HP, Lewis RA, *et al*. The role of the complement system in chronic inflammatory demyelinating polyneuropathy: Implications for complement-targeted therapies. *Neurotherapeutics*. 2022;19:864-873.
86. Davidson AI, Halstead SK, Goodfellow JA, *et al*. Inhibition of complement in Guillain–Barré syndrome: The ICA-GBS study. *J Peripher Nerv Syst*. 2017;22:4-12.
87. Mevorach D, Reiner I, Grau A, *et al*. Therapy with eculizumab for patients with CD59 p.Cys89Tyr mutation. *Ann Neurol*. 2016;80:708-717.
88. van den Bosch A, Fransen N, Mason M, *et al*. Neurofilament light chain levels in multiple sclerosis correlate with lesions containing foamy macrophages and with acute axonal damage. *Neurol Neuroimmunol Neuroinflamm*. 2022;9:e1154.
89. Bischof A, Manigold T, Barro C, *et al*. Serum neurofilament light chain: A biomarker of neuronal injury in vasculitic neuropathy. *Ann Rheum Dis*. 2018;77:1093-1094.
90. Martín-Aguilar L, Camps-Renom P, Lleixà C, *et al*. Serum neurofilament light chain predicts long-term prognosis in Guillain–Barré syndrome patients. *J Neurol Neurosurg Psychiatry*. 2021;92:70-77.
91. Altmann P, De Simoni D, Kaider A, *et al*. Increased serum neurofilament light chain concentration indicates poor outcome in Guillain–Barré syndrome. *J Neuroinflammation*. 2020;17:86.
92. Körtvelyessy P, Kuhle J, Düzel E, *et al*. Ratio and index of neurofilament light chain indicate its origin in Guillain–Barré syndrome. *Ann Clin Transl Neurol*. 2020;7:2213-2220.
93. Mariotto S, Farinazzo A, Magliozzi R, Alberti D, Monaco S, Ferrari S. Serum and cerebrospinal neurofilament light chain levels in patients with acquired peripheral neuropathies. *J Peripher Nerv Syst*. 2018;23:174-177.
94. van Lieverloo GGA, Wieske L, Verhamme C, *et al*. Serum neurofilament light chain in chronic inflammatory demyelinating polyneuropathy. *J Peripher Nerv Syst*. 2019;24:187-194.
95. Broadley J, Seneviratne U, Beech P, *et al*. Prognosticating autoimmune encephalitis: A systematic review. *J Autoimmun*. 2019;96:24-34.